International Journal of Biochemistry and Cell Biology 109 (2019) 40–58

Contents lists available at ScienceDirect

International Journal of Biochemistry and Cell Biology

journal homepage: www.elsevier.com/locate/biocel

PP2ACα deficiency impairs early cortical development through inducing DNA damage in neuroprojenitor cells

Bo Liu[a,b,*,1], Lin Lin[b,f,1], Saima Riazuddin[a], Ahmed Zubair[a], Li Wang[c], Li-Jun Di[c], Ru[illegible][e,f], Ting-Ting Dong[f,g], Chu-Xia Deng[d,***], Wei-Min Tong[d,**]

[a] Department of Otorhinolaryngology Head&Neck Surgery, University of Maryland School of Medicine, Baltimore, USA
[b] University of Macau, Macau, China
[c] Branch of Cancer Research, Jones Hopkins University, Baltimore, USA
[d] National Institute of Neurological Disorders and Stroke, National Institute of Heath, Bethesda, USA
[e] Institute of Biophysics, Chinese Academy of Sciences, Beijing, China
[f] Department of Pathology, Institute of Basic Medical Sciences, Chinese Academy of Sciences. Beijing, China
[g] China Agricultural University, Beijing, China

ARTICLE INFO

Keywords:
Protein phosphorylation
Brain development
DNA damage
Stem cell
Signaling cascade

ABSTRACT

The role of protein phosphatase 2A[illegible] (PP2ACα) i[illegible]ain development is poorly understood. To understand the function of PP2ACα in neurogenesi[illegible] inactivated[illegible]2*aca* gene in the central nervous system (CNS) of mice by Cre/LoxP system and generated the [illegible]Cα defi[illegible]t mice (designated as the *Pp2aca*$^{-/-}$ mice). PP2ACα deletion results in DNA[illegible]ge in neurop[illegible]cells (NPCs), which impairs memory formation and cortical neurogenesis. We fir[illegible]t PP2ACα can directly associate with Ataxia telangiectasia mutant kinase (ATM) and Ataxia tela[illegible]ectasia[illegible]lated kinase (ATR) in neocortex and NPCs. Importantly, the P53 and hypermethylated in can[illegible] (HIC[illegible]) fu[illegible]ion complex, the newly found down-stream executor of the ATR/ATM cascade, w[illegible]translocat[illegible]o nuclei and interact with homeodomain interacting protein kinase 2 (HIPK2) to respon[illegible]DN[illegible]mage. I[illegible]bly, HICI plays a direct transcriptional regulatory role in HIPK2 gene expression. The[illegible]rplay a[illegible]g P53, H[illegible]and HIPK2 maintains DNA stability in neuroprogenitor cells. Taken together, our fi[illegible] high[illegible] role of PP2ACα in regulating early neurogenesis through maintaining DNA stability in neurop[illegible]or cells. P53/HIC/HIPK2 regulation loop, directly targeted by the ATR/ATM cascade, is involved i[illegible]A repair in neuroprogenitor cells.

1. Introduction

Protein kinases and p[illegible]in p[illegible]phatases cooperatively modulate the phosphorylation status[illegible]roteins. [illegible]otein phosphatases, responsible for pro[illegible]phosp[illegible]lati[illegible]play essential roles in the modulation of [illegible]exp[illegible]ion, pro[illegible]ion, differentiation, apoptosis, epithelial to[illegible]enchy[illegible]transition (EMT), signaling transduction and cell cycle prog[illegible]io[illegible]cells (Lyu et al., 2013; Mayer et al., 1991; Santoro e[illegible]1998; Shenolikar, 1994; McCright et al., 1996; Inoue et al., 1999; [illegible]be et al., 1997; Kins et al., 2003; Louis et al., 2011; Kamibayashi an[illegible]umby, 1995; Oliver and Shenolikar, 1998; Alonso et al., 2004; Millward et al., 1999; Sontag et al., 1995; Barford, 1996; Bononi et al., 2011; Mumby and Walter, 1993; Chen et al., 2016; Lucas and Armstrong, 2015; Janssens and Goris, 2001; Okamoto et al., 1996). Previous studies have reported that PP2AC protein positively responds to a series of extra-cellular signals including hormones, growth factors and inflammatory cytokines, regulating cellular metabolism, RNA splicing, transcription, translation, cell cycle progression and oncogenic transformation (Lyu et al., 2013; Mayer et al., 1991; Santoro et al., 1998; Shenolikar, 1994; McCright et al., 1996; Inoue et al., 1999; Kawabe et al., 1997; Kins et al., 2003; Louis et al., 2011; Kamibayashi and Mumby, 1995; Oliver and Shenolikar, 1998; Alonso et al., 2004; Millward et al., 1999; Sontag et al., 1995; Barford, 1996; Bononi et al., 2011; Mumby and Walter, 1993; Chen et al., 2016; Lucas and Armstrong, 2015; Janssens and Goris, 2001; Okamoto et al., 1996).

DNA damage response (DDR) plays a vital role in maintaining the

* Corresponding author at: Department of Otorhinolaryngology Head and Neck Surgery, School of Medicine, University of Maryland, Baltimore, USA.
** Corresponding author at: National Institute of Neurological Disorders and Stroke, National Institute of Heath, Bethesda, USA.
*** Corresponding author at: National Institute of Neurological Disorders and Stroke, National Institute of Heath, Bethesda, USA.
E-mail addresses: boliufhs@umac.mo, lbfhsum@yeah.net (B. Liu), cxdeng@nih.gov (C.-X. Deng), wmtong@nih.gov (W.-M. Tong).
[1] These authors contributed equally to this research work.

https://doi.org/10.1016/j.biocel.2019.01.021
Received 14 November 2018; Received in revised form 25 January 2019; Accepted 29 January 2019
Available online 30 January 2019
1357-2725/

genetic stability of eukaryotic cells. DNA damage can be categorized into two forms: DNA double strand breaks (DSBs) and DNA single strand break (SSB), based on the severity of DNA strand breaks. Following DSBs, NBS1 protein interacts with phosphorylated histone H2AX (γH2AX), promoting the nuclear translocation of the MRE11/RAD50 repair complex to the sites of DSBs, and subsequently activating the Ataxia telangiectasia mutated kinase (ATM) and check point kinase1 (CHK1) cascade (Riches et al., 2008; Lee and Paull, 2005; Difilippantonio and Nussenzweig, 2007; Jazayeri et al., 2008; D' Amours and Jackson, 2002; Stracker and Petrini, 2011; Stiff et al., 2005). Moreover, NBS1 protein also plays a vital role in single-strand break (SSB)-mediated ATR activation and the subsequent phosphorylation of CHK1 in DDR (D' Amours and Jackson, 2002; Lee and Paull, 2005; Difilippantonio and Nussenzweig, 2007; Jazayeri et al., 2008; D' Amours and Jackson, 2002; Stracker and Petrini, 2011; Stiff et al., 2005).

The roles of PP2ACα protein in brain development are poorly understood. To solve this problem, attempt had been made to inactivate *Pp2aca* gene in the central nervous system (CNS) neuronal cells. When *Pp2aca* gene was specifically inactivated in the CNS neuronal cells by Cre/LoxP system, brain phenotype characterized by microcephaly appeared in mice at early postnatal stage. Based on it, we deeply investigated the molecular mechanisms underlying microcephaly, and highlighted that PP2ACα could regulate DNA repair through the ATR-P53-HIC1-HIPK2 cascade in neuronal progenitor cells.

2. Materials and methods

2.1. Mouse model

Mouse experimental procedures were conducted in accordance with NIH guidelines for animal research and were approved by the Institutional Animal Care and Use Committee (IACUC) at University of Maryland School of Medicine. In this study, we used Cre/LoxP system to conditional knock-out *Pp2aca* gene in the CNS neuronal cells of mice. Briefly, prepared for target gene vectors, modified *Pp2aca* gene with two LoxP sites, cultured embryonic stem cells transfected the LoxP-floxed *Pp2aca* gene into embryonic stem cells and generated the LoxP-floxed mice. The LoxP-floxed mice interbred with the Cre transgenetic mice. The genotype of PP2ACα$^{-/-}$ mice was identified by Northern blot and Immunoblotting assay. In this study, we only compared the mice with *Pp2aca* gene floxed (homozygous, fl/fl) and Cre positive (mutant) with the mice that *Pp2aca* gene floxed (homozygous, fl/fl) and Cre negative. *Pp2aca* gene expression was not altered in mice models.

2.2. Primary culture of neuroprogenitor cells (NPCs)

The embryonic (embryonic day 15.5, E15.5) mice were sacrificed, and ependymal tissues were isolated from brain tissues under dissecting microscope. Afterward, tissues were digested by 0.05% trypsin for 15 min, suspension was centrifuged for 15 min at 1000 r/min. Cells were cultured in the NSC expansion medium containing Dulbecco's Modified Eagles's Medium (DMEM)/F12 medium (Gibco/Invitrogen, Carlsbad, CA) with L-glutamine, B27 supplement, 1 × solution of penicillin, streptomycin and fungizone, and basic fibroblast growth factor (bFGF, 20 ng/mL). Cells were maintained at 37 °C in a 5% CO_2 humidified incubator and were subjected to subculture once time every 3–4 days. The purity and specificity of cultured NPCs was confirmed by the immunofluorescent assay of nestin. To induce DNA damage in cells, NPCs were exposed to irradiation IR (4Gy) at distinct time points according to research plan, or treated with 2 mmol HU for 3–5 h. To inhibit PP2ACα gene expression, 20umol okadaic acid was added into culture medium for 48 h.

2.3. Gene expression assay and virus transfection

For miRNA, RNA samples were extracted from the cells treated with TRIzol (Invitrogen). TaqMan miRNA assays (Applied Biosystems) were used to quantify mature miRNA expression. The efficiency of miRNA levels were analyzed by qPCR using Fast SYBR Green Master Mix (Applied Biosystems). For knock-down experiments, Lipofectamine RNAiMAX (Invitrogen) was used to transfect siRNAs into cells.

For gene over-expression assay, we used lentiviral vector system. Briefly, the transfer plasmid encoding insert of interest, two packaging plasmids, envelope plasmid were transferred into 293T cells. After cell culture for 48–72 h, viral supernatants were harvested. Neuroprogenitor cells were infected with viral supernatant for 24 h, at MOI 1000, and selection was begun 48 h after with blasticocin (100 mg/ml) (Invitrogen Life Technologies). All lentiviral vectors were purified and amplified using QIAGEN Plasmid maxi kit (Qiagen, number 12,163). Lentiviral packaging was mediated by ViraPower packaging mix (Invitrogen Life Technologies). For control, empty vector (the transfer plasmid without coding insert of interest), two packaging plasmids and envelope plasmid were transferred into 293T cells, and viral supernatant was harvested. After 48 h, neuroprogenitor cells were infected with viral supernatant.

2.4. Immunoblotting assay, coimmunoprecipitation and GST pulldown assay

Briefly, protein samples extracted from cells or tissues were immersed into RIPA buffer. Protein samples (20–100 μg) were loaded on Bis-Tris gels (Invitrogen), separated by SDS-PAGE, and transferred to nitrocellulose membranes. After 1 h treated in blocking solution (5% non-fat milk in trisbuffered saline, TBS), membranes were incubated with primary antibodies diluted in 5% non-fat milk in TBS/0.1% Tween 20 overnight at 4 °C. After washing by PBS buffer for three times, membranes were incubated with horseradish peroxidase conjugated-secondary antibodies for 1 h at 4 °C. Bands were detected by ECL reagents (Invitrogen). The primary antibodies were listed as following: anti-PP2ACα antibody (1:1000, Cell signaling, Danvers, USA), anti-PP4C antibody (1:1000, Cell signaling, Danvers, USA), anti-PP6C antibody (1:1000, Cell signaling, Danvers, USA), anti-activated Caspase-3 antibody (Asp175) (1:1000, Cell signaling, Danvers, USA), anti-PCNA (PC10) antibody (1:1000, Cell signaling, Danvers, USA), anti-phospho ATR at Ser428 antibody (1:500, Cell signaling, Danvers, USA), anti-ATR antibody (1:1000, Cell signaling, Danvers, USA), anti-ATM (D2E2) antibody (1:1000, Cell signaling, Danvers, USA), anti-phospho ATM at Ser1981 antibody (1:500, Millipore, Massachusetts, USA), anti-phospho CHK2 at Ser383 antibody (1:1000, Cell signaling, Danvers, USA), anti-CHK2 antibody (1:1000, Cell signaling, Danvers, USA), anti-phospho CHK1 at Ser345 antibody (1:500, Cell signaling, Danvers, USA), anti-CHK1 (2G1D5) antibody (1:500, Cell signaling, Danvers, USA), anti-P53 antibody (1:1000, Cell signaling, Danvers, USA), anti-HIC1antibody (1:1000, Cell signaling, Danvers, USA), anti-HIPK2 antibody (1:1000, Cell signaling, Danvers, USA), anti-beta actin antibody (1:2000, Cell signaling, Danvers, USA), anti-GAPDH antibody (1:2000, Cell signaling, Danvers, USA). The corresponding secondary antibodies (1:3000, Cell signaling, Danvers, USA) were used to react with primary antibodies. The final results were obtained from at least three independent experiments.

Anti-Flag and anti-PP2ACα antibodies were coupled to protein G-Sepharose and blocked with BSA. The beads were used to precipitate tagged proteins from cell extracts in RIPA buffer for 1 h at 4C. The beads were washed three times with RIPA buffer, boiled in sample buffer, and electrophoresed on an SDS polyacrylamide gel. After transfer to a PVDF membrane, the bound fraction was assayed for HIC1, HIPK2, ATM and ATR by immunoblotting using corresponding antibodies, respectively.

GST Pulldown assay: GST and GST-HIPK2 were coupled to

glutathione-Sepharose beads and blocked with bovine serum albumin (BSA). Equimo lar amounts of GST or GST fusion proteins were used in pulldown assay. Recombinant PP2ACα was added to HEG100 binding buffer (20 mM HEPES, pH 7.4, 10% glycerol, 100 mM KCl, 1 mM EDTA, and 1 mM dithiothreitol) plus protease inhibitors for 1 h at 4 °C. The beads were washed three times with HEG100 buffer, boiled in sodium dodecyl sulfate (SDS) loading buffer, and electrophoresed on SDS polyacrylamide gel. After transfer to a polyvinylidene difluoride (PVDF) membrane, the bound fraction was detected by immunoblotting using an anti-His antibody (Qiagen).

2.5. Histopathological assay and immunofluorescent assay

Mice were euthanized by carbon dioxide. Brains were fixed in 4% paraformaldehyde, followed by dehydration and paraffin embedding. Immunohistochemical staining was performed on paraffin embedding tissue sections. Briefly, tissue sections were subjected to antigen retrieval under high pressure. Then, tissue sections were immersed into 3% H_2O_2, and then washed by PBS buffer. 5% goat-serum was used to incubate tissue sections for 30 min at room temperature. Then sections were incubated with primary antibody overnight at 4 °C, and then sections were washed by PBS buffer for three times. Incubated with the corresponding secondary antibody against primary antibody for 1 h at 4 °C, sections were developed by DAB reagent. Stained sections were observed under light microscope (Zeiss Axioskop). Images were captured with identical exposure settings. The primary antibodies: anti-PP2ACα antibody (1:400, Cell signaling, Danvers, USA), anti-Nestin antibody (1:500, Cell signaling, Danvers, USA), anti-PH3 antibody (1:200, Cell signaling, Danvers, USA) and anti 8-OHdG antibody (1:400, Cell signaling, Danvers, USA). The corresponding secondary antibodies (1:1000, Cell signaling, Danvers, USA) were used to react with pri antibodies.

Primarily cultured NPCs were grown on cover slips. Cover slips w rinsed with PBS, then fixed in 100% methanol for 10 min and washed PBS. Cover slips were incubated in blocking solution nal goa serum in 0.1% TBS-Tween-20) for 1 h at room te rature d then kept overnight at 4°C with anti-PP2ACα anti (1:4 Cambridge, Britain), anti-γH2AX (1:500, Cell mar vers, anti-SMCI antibody (1:400, Abcam, Ca dge, Bri anti-phosphorylated ATR (Ser428) (1:400, Cell ng, Danver A), anti-HICI antibody (1:500, Abcam, Ca dge tain) and ti-HIPK2 antibody (1:400, Abcam, Cambri e, Britain). r rinses with 0.1% TBS-Tween-20, cells were inc d for 1 h at ro mperature with the corresponding secondar tibodi (1:500, Cell signaling, Danvers, USA) diluted in 4% norm oat s n in TBS. Nuclei was stained by DAPI. Digitized images of were c ned with an all-in-one fluorescence micr system eiss oskop). Images were captured with iden exp re setti

2.6. Animal b ior

The Barnes Ma t was performed using a standard apparatus. Four-month-old mice e transported from animal facility to the center of the platform via a closed starting chamber where they remained for 10 s prior to exploring the maze for 3 min. Mice failing to enter the escape box within 3 min were guided to the escape box by the researchers, and the latency was recorded as 180 s. Before the next trial, mice were allowed to remain in the escape box for 1 min. Two trials per day during 4 consecutive days were performed. All trials were recorded by video camera and analyzed with ANY-maze video tracking software (Stoelting Co, Wood Dale, USA).

2.7. Comet assay, focus formation, cell imaging assay and ChIP assay

Comet assay was carried out according to the manufacturer's instruction (Trevigen, USA). At least 1200 nuclei per field were counted and scored. The number of nuclei with the comet tails was counted in a randomly selected area under a fluorescent assay microscope. Comet score software (Autocomet) automatically determined the tail length using a built-in algorithm for comet scoring.

To induce focus formation, cells were plated onto poly-D-lysine-coated coverslips, treated with or without 2 mM HU for 3–5 h, and fixed. Briefly, cells were washed once in PBS with 1 mM glycerolphosphate, 1 mM Na_3VO_4, 10 mM NaF and 1 mM PMSF, and further treated with a hypotonic lysis solution containing 10 mM Tris-HCl pH 7.4, 2.5 mM $MgCl_2$, 1 mM PMSF, 1 mM glycerolphosphate, 1 mM Na_3VO_4, 10 mM NaF and 0.5% Nonidet P-40 for 8 min on ice. Subsequently cells were fixed in ice-cold acetone-methanol (1:1) for 30 min on ice. The slides were then incubated with appropriat imary antibody in TBST containing 5% non-fat dried milk. Slide ted in Vectashield mounting medium with DAPI (Ve Laborato and visualized under a Zeiss Axioskop fluorescence oscope equ ed with a CCD imaging system (IP Lab Spectr A ce th at lea en distinct foci in the nucleus was scored a cus positiv d ast 150 cells per staining were analyzed.

For ChIP assay, cells fi oss linked with 1% formaldehyde. Chromatin was pr ed f ese fo dehyde cross-linked cells and fragmented n average of 400 bp by sonication. ChIP-Seq experim performed sing the antibody against HIC1 (1:400, Cel ignal Davers, USA). Briefly, 2 μg of the antibody binded to 20 μl of Dyn ds protein A beads at room temperature for 1 h ation. Added matin mixture to the beads + antibody, in ated at 4 °C for overnight with rotation. Then washed, reversed cr -link, prec ted ChIP DNA. Then real-time PCR analysis was pe med.

2.8. Luc activity assay

uciferase activity assay, pGL3B vector containing different promoter sequences were transfected into cells. All transfections were performed with Lipofectamine™ 2000 (Invitrogen). After 24 h incubation, luciferase activity was assessed with the Dual-Luciferase Reporter Assay Kit (Promega).

2.9. Statistical assay

The final data shown in figures were presented as mean values and standard deviation (S.D.) of separate experiments ($n \geq 3$). Student's *t*-test was used to compare the differences between two groups. 2-way ANOVA assay was used to compare more than two groups. Statistical calculations were performed using SPSS software (version 19.0, SPSS, Chicago, IL). P value of less than 0.05 ($p < 0.05$) was considered significant.

3. Results

3.1. The generation of *Pp2acα*$^{-/-}$ mice

To elucidate the role of PP2ACα protein in brain development, we inactivated *Pp2acα* gene in the CNS neuronal cells by Cre/LoxP system. Due to its essential role in brain development, null mutation of *Pp2acα* gene in mice lead to embryonic lethality. Although mice with the hypomorphic mutation of *Pp2acα* gene were viable, they did not exhibit obvious brain phenotype. When *Pp2acα* gene was specifically inactivated in the CNS neuronal cells by Cre/LoxP system, brain phenotype characterized by microcephaly appeared in mice at early postnatal stage. The genotype of the PP2ACα deficient mice (designated as the *Pp2acα*$^{-/-}$ mice) was confirmed by immunoblotting assay (Fig. 1a and b). However, PP2ACα deletion did not impair PP4C and PP6C protein expressions (Fig. 1a and b).

To confirm the deletion of *Pp2acα* gene in the CNS neuronal cells, we first primarily cultured neuroprogenitor cells from the *Pp2acα*$^{-/-}$

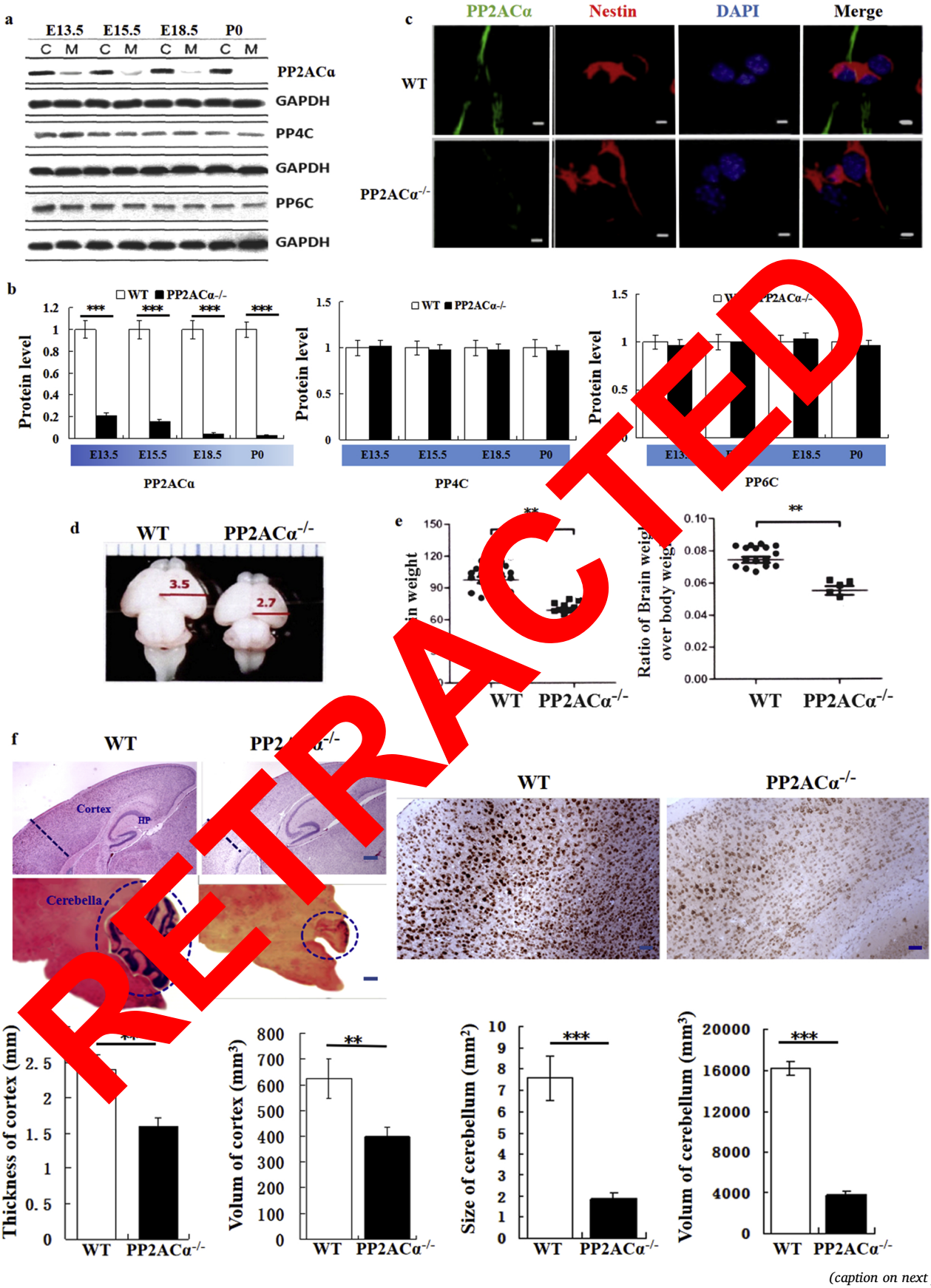

(caption on next page)

Fig. 1. PP2ACα deletion results in microcephaly.
a) Protein expression levels of PP2ACα, PP4C and PP6C in the whole brain tissue lysates obtained from the *Pp2aca*$^{-/-}$ mice (n = 20) and the WT mice (n = 20) at embryonic day 13.5, 15.5, 18.5 and postnatal day 0. C: WT mice; M: *Pp2aca*$^{-/-}$ mice. **b)** Quantitation of protein levels of PP2ACα, PP4C and PP6C. ***$p < 0.001$ VS. WT. *t*-test. **c)** Immunofluorescent assay of co-expressions of PP2ACα and nestin in the cytoplasm of neuroprogenitor cells. Alexa staining (green), phalloidin staining (red), DAPI staining (blue). Scale bar represents 5 μm. **d)** Gross morphological features of the *Pp2ac*$^{-/-}$ mouse brain and the WT mouse brain at postnatal day 0 (P0). **e)** Left: evaluation of brain weight for the *Pp2ac*$^{-/-}$ mice (P0) and the age-matched WT mice; Right: ratio of brain weight over body weight. ***$p < 0.001$ VS. WT. *t*-test, n = 10. **f)** Morphological features of cerebral cortex and cerebella in the *Pp2aca*$^{-/-}$ mouse and the WT mouse at postnatal day 21 (P21). HE staining (left) and Immunohistochemical assay of NeuN (right). Scale bar represents 200 μm. **g)** Evaluation of cortical thickness, volume, cerebellar size and volume by stereological assay. **$p < 0.01$ VS. WT, ***$p < 0.001$ VS. WT, *t*-test, n = 20. Bar graphs represent means ± S.D. of experimental triplicates.

mice (at embryonic day 15.5, E15.5) and the age-matched Wild Type (WT) mice. Subsequently, we measured the co-expressions of nestin and PP2ACα in neuroprogenitor cells by immunofluorescent assay. As we expected, PP2ACα was absent in the nestin-positive neuroprogenitor cells from the *Pp2aca*$^{-/-}$ mice. In contrast, PP2ACα and nestin were co-expressed in the cytoplasm of the WT neuroprogenitor cells (Fig. 1c).Taken together, these results indicated that *Pp2aca* gene had been deleted in the CNS neuronal cells by Cre/LoxP system.

3.2. PP2ACα deletion causes to microcephaly

Macroscopically, the *Pp2aca*$^{-/-}$ mice exhibited microcephaly at early postnatal stage (at postnatal day 0, P0). The maximum width of brain hemisphere was 2.7 ± 0.51 for the *Pp2aca*$^{-/-}$ mice, compared with 3.5 ± 0.73 for the age-matched WT mice ($P = 0.030$, Fig. 1d). Average brain weight was 70.2 ± 14.5 for the *Pp2aca*$^{-/-}$ mice, compared with 95.7 ± 20.3 for the WT mice ($P = 0.0025$, Fig. 1e). The ration of brain weight over body weight was 0.051 ± 0.016 for the *Pp2aca*$^{-/-}$ mice, compared with 0.078 ± 0.011 for the age-matched WT mice ($P = 0.0080$, Fig. 1e).

In mouse brain, cerebral cortex is formed in embryo. How mature cerebellar structure will be formed at postnatal stage (us from postnatal day 0 to postnatal day 21). As a consequence of PP2A deletion, cortex and cerebella both exhibited defective morphologic features. Cerebral cortical structures developed com ut con tained decreased neuronal cells relative to the WT hile P Cα-de- ficient cerebella exhibited severe maldevelopmen aracte the disorganized and incomplete histological lay (Fi

As analyzed by stereological deter ation, c ral cortical thickness and volume were 1.6 ± 0. and 392 ± mm^3 respectively for the *Pp2aca*$^{-/-}$ mice pos l day 21, P 1), compared with 2.4 ± 0.43 mm and 10 ± 87 m espectively for the age-matched WT mice ($P =$ 041, 0.0030, re tively, Fig. 1g). Cerebellar size and volum ere 1.8 ± 0.33 mm and 3978 ± 457 mm^3 respectively for th 2acα mice at P21, compared with 7.6 ± 2.3 mm^2 and 16,27 30 mm^3 espectively for the age-matched WT mi 0.00 0.0 7, respectively, Fig. 1g). Overall, these pho cal alt indicated the essential regulatory role P2ACα brain dev opment.

3.3. PP2ACα de results in neuroprogenitor cell growth retardation

The mitotic cells id fied by PH3 (phosphorylated-histone protein 3) were decreased by 31.5% (Fig. 2a, e), and the incorporation rates of BrdU into mitotic cells was decreased by 33.7% (Fig. 2b, e), in the PP2ACα deficient neocortex (at embryonic day 13.5, E13.5), compared with those in the age-matched WT neocortex ($p < 0.05$). To confirm defective proliferation was localized in neurons, we measured the EdU incorporation rates in neuroprogenitor cells. As expected, PP2ACα deletion resulted in decreased EdU incorporation into cells ($p < 0.05$, Fig. 2c and e).

Neuroprogenitor cells formed the characteristic neurospheres on culture plates in vitro. The neurospheres formed by PP2ACα deficient cells exhibited proliferation deficits, starting at post culture day 1 (P1), and becoming evident at post culture day 2 (P2) ($p < 0.05$, Fig. 2d and e).

As shown in Fig. 2f and g, TUNEL assay revealed a striking increase in apoptotic cells in PP2ACα deficient neocortex (E13.5), compared with the age-matched WT neocortex (p < 0.001). in vitro study, apoptotic response was confirmed in th eficient neuroprogenitor cells, as evidenced by the in sed immu activity of activated Caspase3 ($p < 0.001$, Fig. 2h i), implying at PP2ACα deletion resulted in neuroprogeni cell g th retard on.

3.4. PP2ACα maintains c ive int y in ad ce

We assumed th p2a mice p suffer from cognitive impairments, due ne wide s d n onal apoptosis in neocortex. Indeed, the d ained from water maze (MWM) test confirmed this sumpt The adult *Pp2aca*$^{-/-}$ mice (at postnatal month 4) swam longer and c icated paths in water maze, compared with the tched WT m ($p < 0.001$, Fig. 3a and b), implying PP Cα deficiency in neocortex impaired cognitive integrity in adult m

3.5. ACα d on induces DNA damage in neocortex and neuropro cells

ive deficit originates from pathological changes in neuronal morphology and function, and several of these alterations occur in the disease associated with the change in DNA integrity and stability (Riches et al., 2008; Lee and Paull, 2005; Difilippantonio and Nussenzweig, 2007). The role of PP2ACα in DNA repair was not reported in previous studies. Here, our data first demonstrated that PP2ACα deletion triggered DNA damage response in neocortex at E13.5, as evidenced by the increased neuronal cells positively reactive with SMC1 and 8-OHdG (two markers for DNA damage) in neocortex ($p < 0.001$, Fig. 3c and d).

To confirm the occurrence of DNA damage in neuronal cells, we performed comet tail assay in the neuroprogenitor cells (subjected to 4Gy irradiation stimuli for 0 h and 36 h, respectively). Due to impaired DNA repair mechanism, comet tails still appeared in the PP2ACα-deficient cells, at 36 h post IR stimuli. In contrast, comet tails could hardly be recognized in the WT cells ($P < 0.001$, Fig. 3e and f).

To validate this result, we first treated the two group cells with Hydroxyurea (HU), extracted nuclear protein samples, and subsequently measured the immunoreactivity of phosphorylated-histone H2AX (γH2AX). Interestingly, γH2AX protein expression level was time dependent upon HU treatment ($P < 0.001$, Fig. 3g and h). In contrast to the WT, PP2ACα deficiency resulted in the enhanced γH2AX immunoreactivity ($P < 0.001$, Fig. 3g and h). Overall, these results indicated that PP2ACα was involved in DNA repair mechanism in neuroprogenitor cells.

3.6. PP2ACα activates the ATR/ATM cascade

To study the uncharacterized functions of PP2ACα in DNA repair, phosphorylation profiles of the proteins, confirmed as the key components of a series of signaling cascades, were measured in scrambled (mock) and PP2ACα-deficient neuroprogenitor cells. Pathway phospho ChIP (containing 1318 specific antibodies responsible for identifying the 679 phosphorylation sites in 432 signaling transduction-relevant

proteins) was used in this experiment. Notably, global assay revealed that several kinases (Hedgehog, Jak/Stat, Notch, Wnt, p38MAPK, JNK, mTOR, NF-κB, MST1/2 and ATR) showed statistically differences in phosphorylation activities between the two group cells. Among these kinases, ATR phosphorylation activity was altered most prominently (increased by 73.1% relative to the WT).

This finding was confirmed in the protein extracts obtained from the neocortex of the *Pp2acα*$^{-/-}$ mice at E15.5. The phosphorylation activity of ATR (S428) (Fig. 4a, b, e and f), but not that of ATM (S1981) (data not shown), was profoundly up-regulated in the PP2ACα deficient neocortex. And ATR phosphorylation activity was gradually enhanced in cells from 0 to 24 h post IR (4Gy) stimuli (Fig. 4c and d).

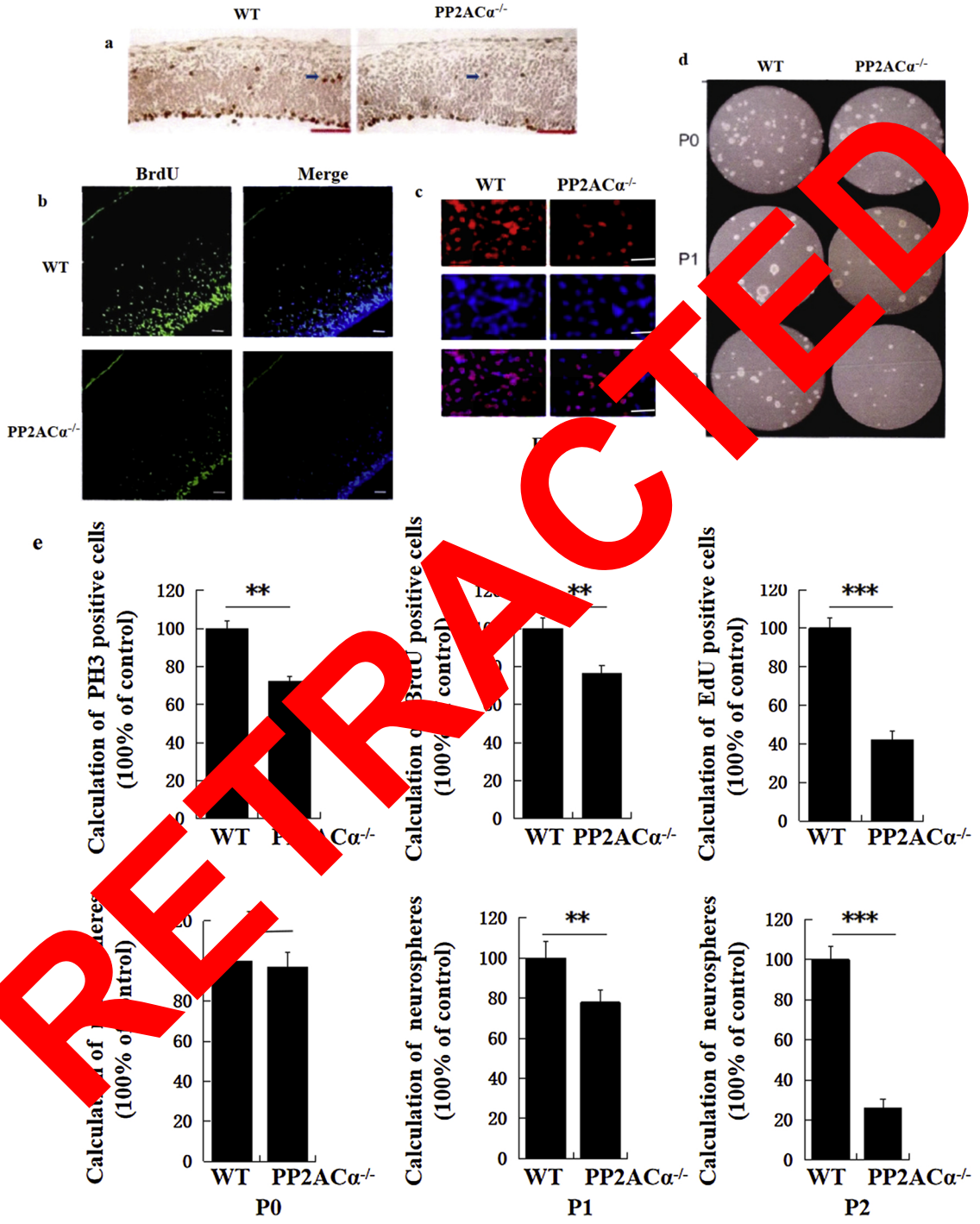

Fig. 2. PP2ACα deletion inhibits the growth of neuroprogenitor cells.
a) Immunohistochemical assay of PH3 on brain tissue sections. Arrow points to the location of PH3 reactive neurons. Scale bar represents 200 μm. **b)** Incorporation of BrdU into neocortex tissues at E13.5. Alexa staining (green). **c)** EdU incorporation assay in neuroprogenitor cells. EdU (red), DAPI (blue). Scale bar = 200 μm. **d)** Neurospheres formed by neuroprogenitor cells at post culture day 0 (P0), day 1 (P1) and day 2 (P2). **e)** Percentage of PH3 positive cells, percentage of BrdU positive cells, percentage of EdU positive cells, calculation of neurospheres at P1 and P2. $^{**}p < 0.01$ VS. WT, $^{***}p < 0.001$ VS.WT. NS: no statistical differences. *t*-test, n = 10. **f)** TUNEL staining in neocortex. Alexa staining (green), API staining (blue). Scale bar represents 50 μm. **g)** Quantitation of TUNEL positive cells in neocortex. $^{***}p < 0.001$ VS. WT, *t*-test, n = 10. **h)** Immunoblotting assay of activated-Caspase3 in the protein lysates obtained from neuroprogenitor cells. **i)** Quantitation of activated Caspase3 protein level. $^{***}p < 0.001$ VS. WT, *t*-test, n = 10. Bar graphs represent means ± S.D. of experimental triplicates.

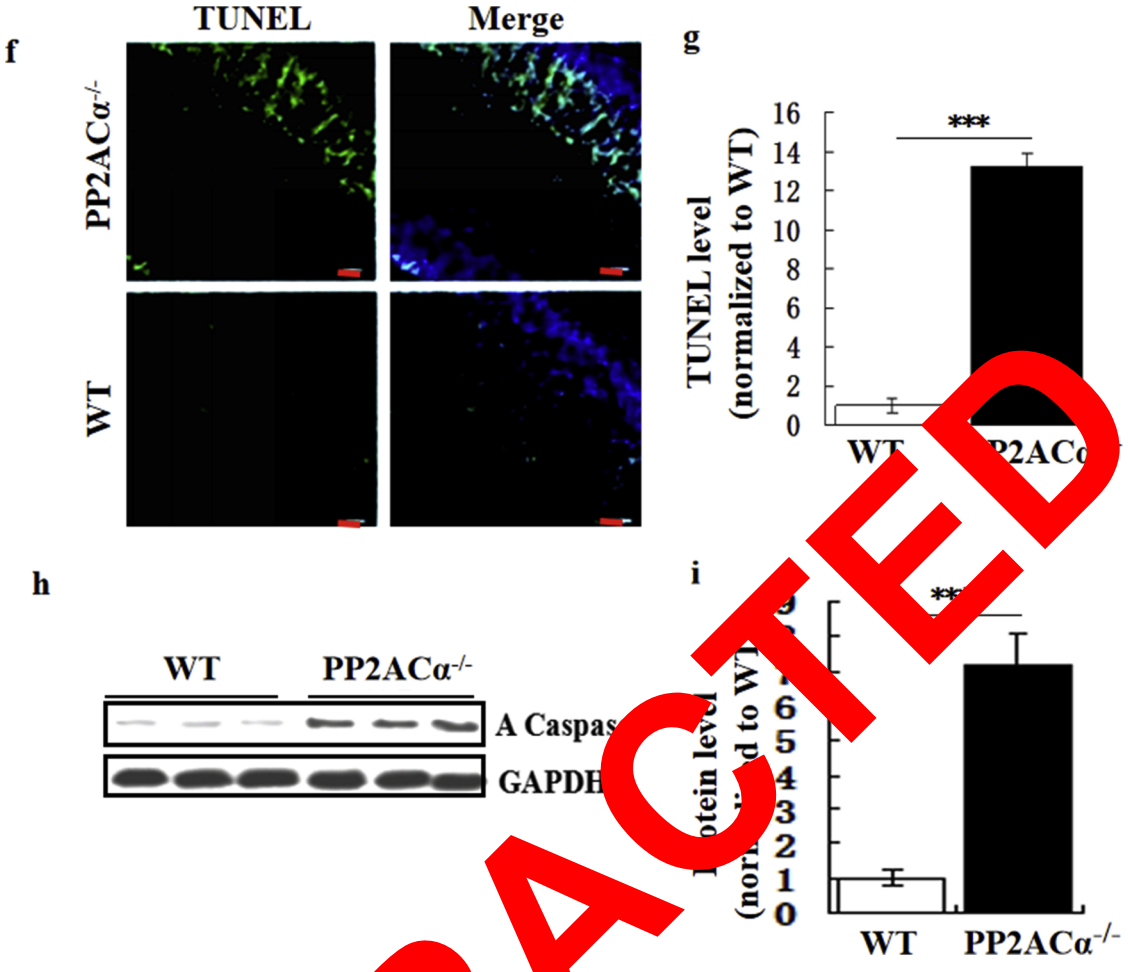

Fig. 2. (*continued*)

As a consequence of the ATR cascade initiat… activity of CHK1 (down-stream transducer … ATR) … enhanced accordingly, both in the PP2ACα deficient … ortex and … progenitor cells (Fig. 4e and f). in vitro study, … lation activ… of ATR (S428) and CHK1 (S345) were time d…pende… …n IR stimuli (Fig. 4g and h). Since the ATR/CHK1 ca… can sense a… pair single strand break (SSB), therefore, PP2A… deletion mainly i…ced SSB in neuroprogenitor cells, which i…ated th… R/CHK1 cascade, but not alter the ATM/CHK2 cascade.

To validate this …ult, P-… (S428) …munoreactivity was evaluated in the WT … genito… …'s … oplasmic extracts, 72 h after transfection w… PP2AC… siRNA o… …ambled siRNA. Upon DNA damage stimu… Gy IR… …of PP2ACα resulted in a clear upregulation of P-A… 28) (Fig. …a and c). PP2ACα inhibitor, okadaic acid (20umol for … could efficiently suppress PP2ACα protein expression (Fig. 5b and … -ATR (S428) immunoreactivity was increased in the WT neuroprogeni…or cells treated with okadaic acid (Fig. 5b and c). In contrast, P-ATR (S428) immunoreactivity was significantly inhibited in the WT neuroprogenitor cells over-expressing PP2ACα (Fig. 5a and b).

PP2ACα deficiency initiated the ATR/Chk1 cascade. However, it could not exclude the possibility that PP2ACα also modulated ATM phosphorylation in the cells with double strand breaks (DSBs). To verify this assumption, we measured P-ATM (S1981) immunoreactivity in the cytoplasmic extracts from the WT neuroprogenitor cells, subjected to PP2ACα siRNA transfection, or treated with 20umol okadaic acid for 48 h. Under the condition of high IR dose (10Gy) stimuli, PP2ACα down-regulation promoted the activity of P-ATM (S1981) in cells (Fig. 5d and e). In the subsequent study, we infected the WT neuroprogenitor cells with recombinant lentiviral vectors carrying full-length PP2ACα, treated cells with high dose IR, and then measured P-ATM (S1981) immunoreactivity again. Intriguingly, over-expression of PP2ACα contributed to the compromised phosphorylation activity of ATM (S1981) (Fig. 5d and e). Over, it concluded that PP2ACα was responsible for the modulation of de-phosphorylation of both ATM and ATR in neuronal stem cells. Activation of ATM or ATR would be controlled by the level of DNA damage.

3.7. Identification of ATR and ATM as endogenous PP2ACα-associated proteins

Whether PP2ACα could interact with ATM and/or ATR was unknown. To verify protein-protein interactions, we performed the coimmunoprecipitation assay in the cytoplasmic extracts from WT neuroprogenitor cells using the antibody against PP2ACα. Notably, PP2ACα could either coimmunoprecipitate with endogenous ATR or endogenous ATM (Fig. 5f). When we induced *Atm* or *Atr* gene silence by siRNA interference in neuroprogenitor cells, two proteins' interactions with PP2ACα could not be detected in cytoplasmic extracts (Fig. 5g). Confocal assay revealed the co-localization of PP2ACα, ATR and ATM in the perinuclear regions of neuroprogenitor cells (Fig. 5h).

However, the data obtained from cellular extracts only demonstrated physical contacts between these proteins, but not reveal whether their interactions was direct. To confirm the direct protein-protein interactions, the purified Flag-PP2ACα protein was synthesized. It coimmunoprecipitated with the recombinant GST-fused aminoterminal portion of ATM or ATR. Flag-antibody resin was identified to coimmunoprecipitate with the recombinant Flag-PP2ACα, GST-ATM and

GST-ATR, respectively. However, Flag-PP2ACα could not coimmunoprecipitate with GST alone, implying that PP2ACα could directly bind to ATM or ATR aminoterminus in the WT neuroprogenitor cells (Fig. 5i). Taken together, these results first identified ATM and ATR as endogenous interactive proteins for PP2ACα.

3.8. HIC1 and P53 function complex up-regulates HIPK2 upon DNA damage stimuli

ATR-Chk1 initiation will block cell cycle progression through up-regulating P53 that triggers apoptotic response in the cells with

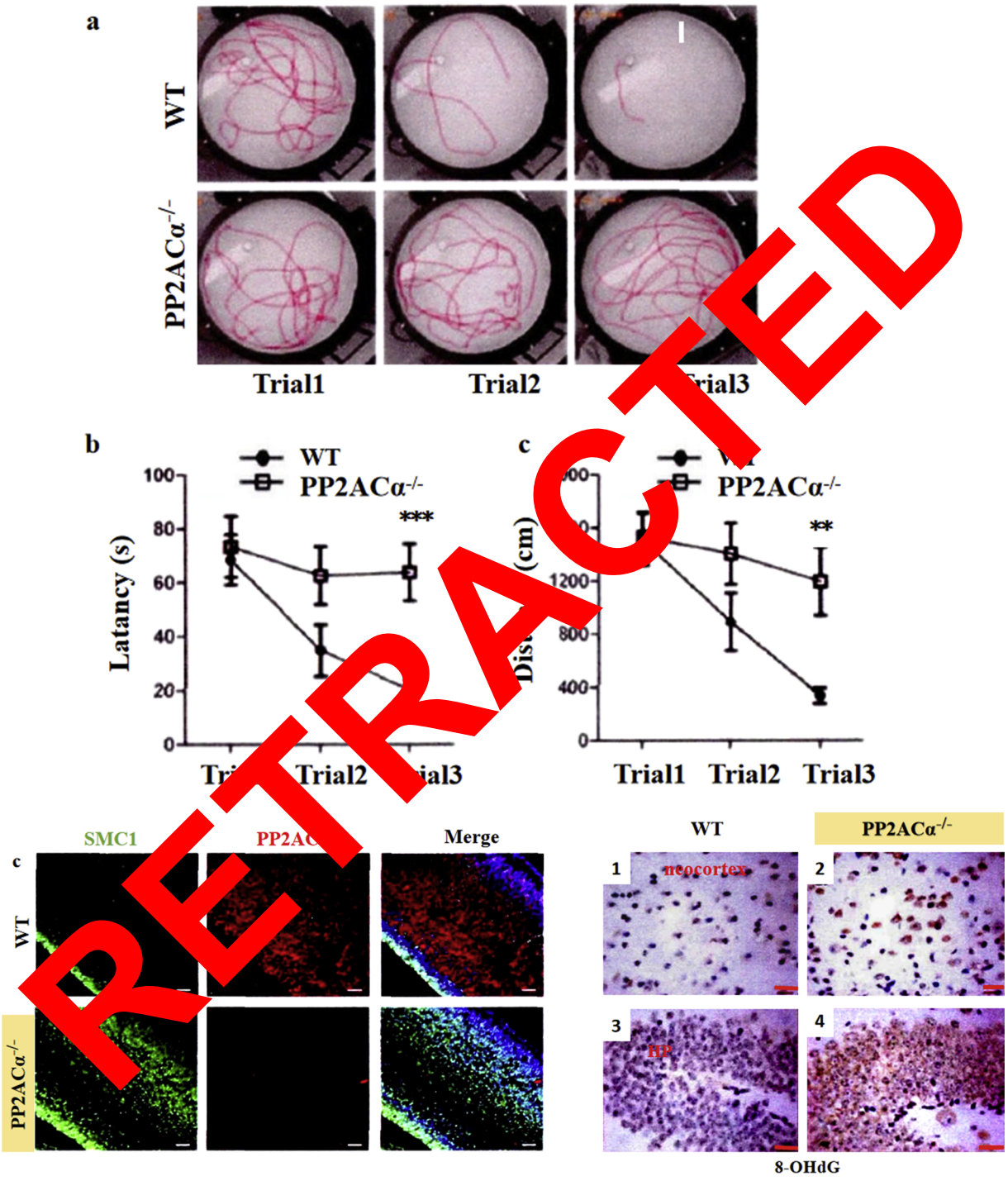

Fig. 3. PP2ACα deletion impairs cognition in adult mice.
a) Morris water maze test. Graphs showing swimming path in water maze. In trial 1, mice were not received systematically swimming training. In trial 2 and 3, mice received systematically swimming training. **b)** Latency (left) and distances (right). $^{**}p < 0.01$ VS. WT, $^{***}p < 0.001$ VS. WT, *t*-test, n = 6. **c) Left:** immunofluorescent assay of SMC1 and PP2ACα in neocortex. Alexa staining (green), phalloidin staining (red), DAPI staining (blue). Scale bar represents 50 μm. **Right:** immunohistochemical assay of 8-OHdG in neocortex and hippocampus. HP: hippocampus. Scale bar represents 20 μm. **d)** Quantitation of immunoreactivity of SMC1, and calculation of 8-OHdG reactive neurons. $^{***}p < 0.001$ VS. WT, *t*-test, n = 10. **e)** Comet tail assay in neuroprogenitor cells at 0 h and 36 h post irradiation (IR) stimuli. **f)** Calculation of the cells with comet tails. $^{***}p < 0.001$ VS. WT, *t*-test, n = 10. **g)** Immunoblotting assay of γH2AX in the protein lysates from neocortex at 0 h, 12 h, 24 h and 48 h post 4Gy IR stimuli. **h)** Quantitation of immunoreactivity of γH2AX. $^{**}p < 0.01$ VS. WT, $^{***}p < 0.001$ VS. WT, *t*-test, n = 10. Bar graphs represent means ± S.D. of experimental triplicates.

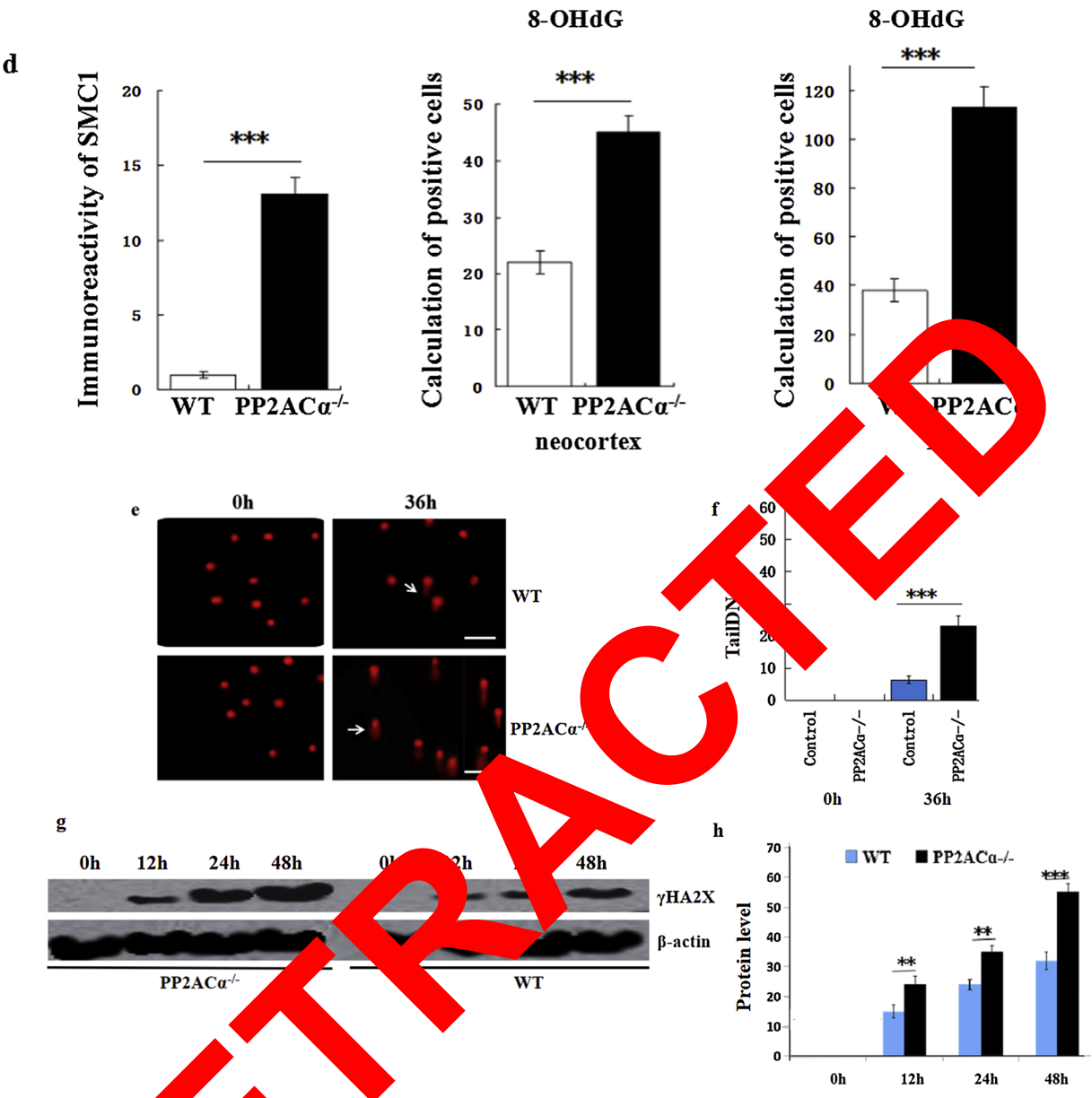

Fig. 3. (*continued*)

unrepaired DNA strand brea… Ponso e…, 2004; Millward et al., 1999; Sontag et … Barfo… 99…Bononi et al., 2011; Mumby and Walter, 1… Che… et al., 2… Lucas and Armstrong, 2015; Janssens an… is, 20… identify P53-interacting proteins, the cell clones stably e… …d P53 protein were constructed. TAP was purified in th… …lei extracts from the cells with over-expression of P53 revealed severa… …oteins that specifically copurified with P53. Putative P53-interacting proteins were further confirmed by mass-spectrometric (MS) assay. Among the interacting proteins identified by MS assay, HIC1 and HIPK2 were selected as potential target proteins, based on a combined Mascot score of 355 in MS assay.

To validate this finding in cells, coimmunoprecipitation analysis was performed in the nuclei extracts from WT neuroprogenitor cells, using the antibody against P53. Upon DNA damage stimuli (4Gy IR), HIC1 and HIPK2 both could coimmunoprecipitate with P53. And HIC1 could independently coimmunoprecipitate with HIPK2 alone (Fig. 6a).

In agreement with coimmunoprecipitation analysis, confocal analysis revealed that P53 and HIC1 were co-expressed in the cytoplasm of normal neuroprogenitor cells. Under the condition of DNA damage, resulting from HU stimuli, P53 and HIC1 were both translocated into nuclei, and they formed foci at the sites of DNA strand breaks (Fig. 6b). In addition, PP2ACα deletion promoted the nuclear translocation of P53-HIC1 function complex, and induced them to form strong foci (Fig. 6b).

Consistently, immunoblotting assay revealed the enhanced protein levels of P53 and HIC1 in the cells suffering from DNA damage (Fig. 6c and d). However, we did not find that PP2ACα could immunoprecipitate with HIC1 and P53, implying that PP2ACα could modulate P53 activity through the ATR-Chk1 cascade.

To investigate whether P53 and/or HIC1 could directly target HIPK2, we induced *P53* gene or *Hic1* gene silence (by siRNA) in WT neuroprogenitor cells, and measured HIPK2 protein expression level. Upon DNA damage stimuli (4Gy IR), knock-down of P53 by siRNA interference inhibited the protein expression of HIPK2 in nuclei extracts. Similar results could be obtained from the cells treated with P53 inhibitor: pifithrin-α (PFTα, 20umol, 48 h) (Fig. 6e and f).

Importantly, HIC1 deficiency resulted in the compromised HIPK2 protein expression. Upon DNA damage stimuli (4Gy IR), HIPK2 immunoreactivity was dramatically reduced in the cells treated with PFTα (Fig. 6e and f), implying that P53 and HIC1 cooperatively maintained

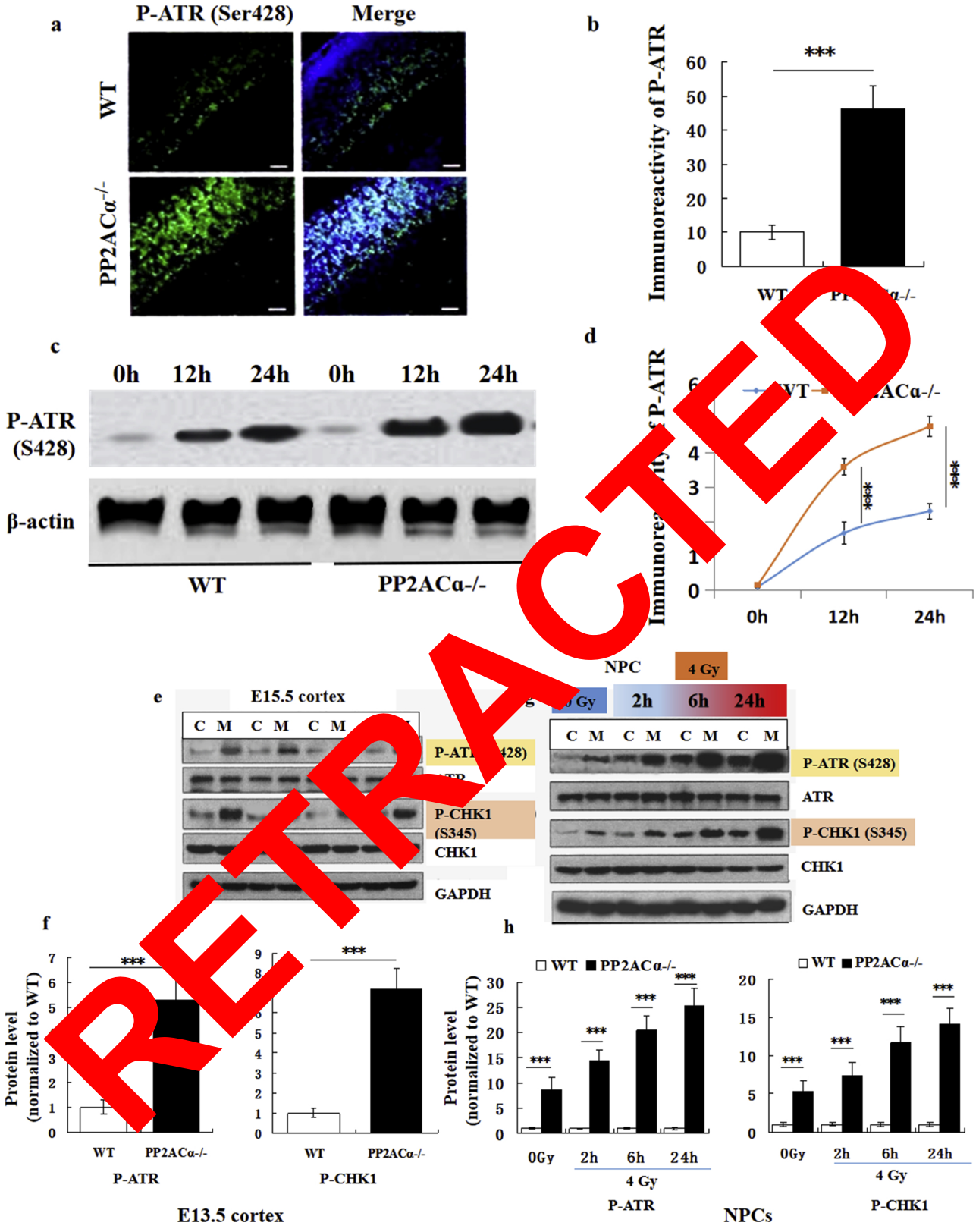

Fig. 4. PP2ACα deletion initiates the ATR/Chk1 cascade.
a) Immunofluorescent assay of P-ATR (S428) in neocortex. Alexa staining (green), DAPI staining (blue). Scale bar represents 50 μm. **b)** Quantitation of P-ATR (S428). ***$p < 0.001$ VS. WT, *t*-test, n = 10. **c)** Immunoblotting assay of P-ATR (S428) in the protein lysates from neocortex at 0 h, 12 h and 24 h post 4Gy IR stimuli. **d)** Quantitation of P-ATR (S428). ***$p < 0.001$ VS. WT, *t*-test, n = 10. **e)** Immunoblotting assay of P-ATR (S428), ATR, P-CHK1 (S345) and CHK1 in the protein lysates from neocortex. M: PP2ACα$^{-/-}$ group. C: WT group. **f)** Quantitation of P-ATR (S428) and P-CHK1 (S345). ***$p < 0.001$ VS. WT, *t*-test, n = 10. **g)** Immunoblotting assay of P-ATR (S428), ATR, P-CHK1 (S345) and CHK1 protein levels in the lysates obtained from the neuroprogenitor cells treated with or without 4Gy IR stimuli (2 h, 6 h and 24 h). **h)** Quantitation of P-ATR (S428) and P-CHK1 (S345). ***$p < 0.001$ VS. WT, *t*-test, n = 10. Bar graphs represent means ± S.D. of experimental triplicates.

the steady-state of HIPK2 protein expression.

In order to investigate the impact of ATR on P53 phosphorylation, we inhibited the ATR cascade (by pharmacological agent: 10umol AZ20 for 48 h or siRNA-mediated *Atr* gene knock-down) in neuroprogenitor cells, and measured P53 phosphorylation activity. As shown in Fig. 6g and h, inhibition on ATR signaling resulted in the compromised P53 phosphorylation activity.

The cells with unrepaired DNA strand breaks will be induced to death, usually in the form of apoptosis. P53 functions as a classical regulator in apoptotic response (Santoro et al., 1998; Shenolikar, 1994;

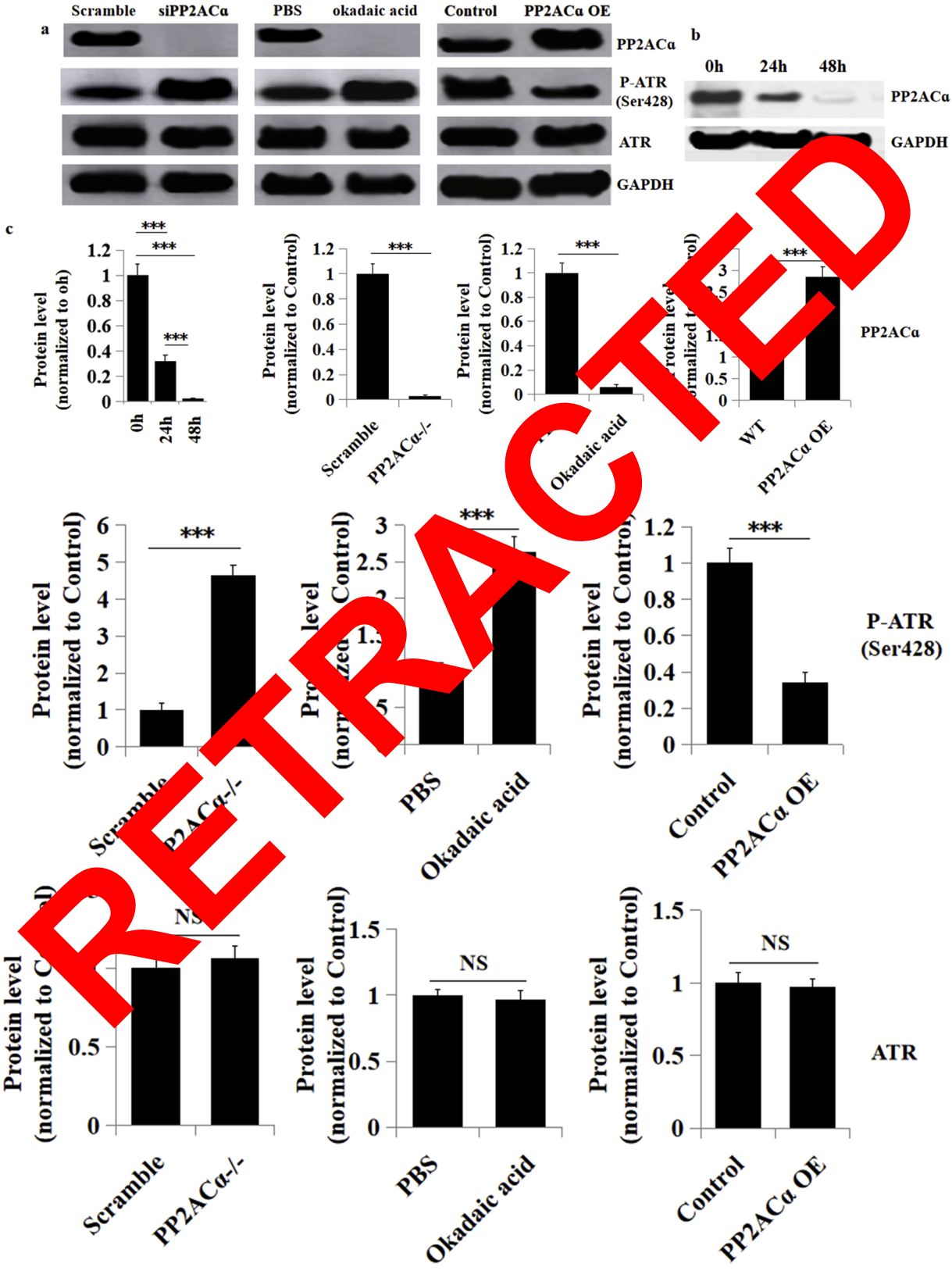

(caption on next page)

Fig. 5. Interactive proteins with PP2ACα in neuroprogenitor cells.
a) Immunoblotting assay of PP2ACα and P-ATR (S428) protein levels in the cytoplasmic lysates of the WT neuroprogenitor cells. siPP2ACα: siRNA-mediated PP2ACα knock-down; PP2ACα OE: PP2ACα over-expression. **b)** Immunoblotting assay of PP2ACα in the WT neuroprogenitor cells treated with okadaic acid. **c)** Quantitation of PP2ACα and P-ATR (S428) protein levels in cells. ***$p < 0.001$ VS. WT, *t*-test, n = 10. **d)** Immunoblotting assay of PP2ACα and P-ATM (S1981) protein levels in the WT neuroprogenitor cells subjected to 10Gy IR. siPP2ACα: siRNA-mediated PP2ACα knock-down; PP2ACα OE: PP2ACα over-expression. **e)** Quantitation of PP2ACα and P-ATM (S1981) protein levels in cells. ***$p < 0.001$ VS. WT, *t*-test, n = 10. **f)** Immunoprecipitation assay of PP2ACα/ATR and PP2ACα/ATM in the cytoplasmic extracts from the WT neuroprogenitor cells subjected to 4Gy IR. PI: preimmune serum (from the same species corresponding to primary antibody). Input: input material. **g)** Co-immunoprecipitation assay of PP2ACα/ATM and PP2ACα/ATR were measured in the cytoplasmic extracts from the treated WT neuroprogenitor cells. **h)** Immunofluorescent assay of ATM and ATR in the cytoplasm of the treated WT neuroprogenitor cells. Alexa staining (green), phalloidin staining (red), DAPI staining (blue). Scale bar represents 2 μm. **i)** *In vitro* binding assay with immobilized, recombinant Flag-PP2ACα protein and recombinant GST protein or with GST-ATM protein or with GST-ATR protein. Immunoblots of eluates with GST (top) or PP2ACα (bottom). Input and GST proteins were used for interaction assay. Shown is a representative blot of three independent experiments with similar results. Bar graphs represent means ± S.D. of experimental triplicates.

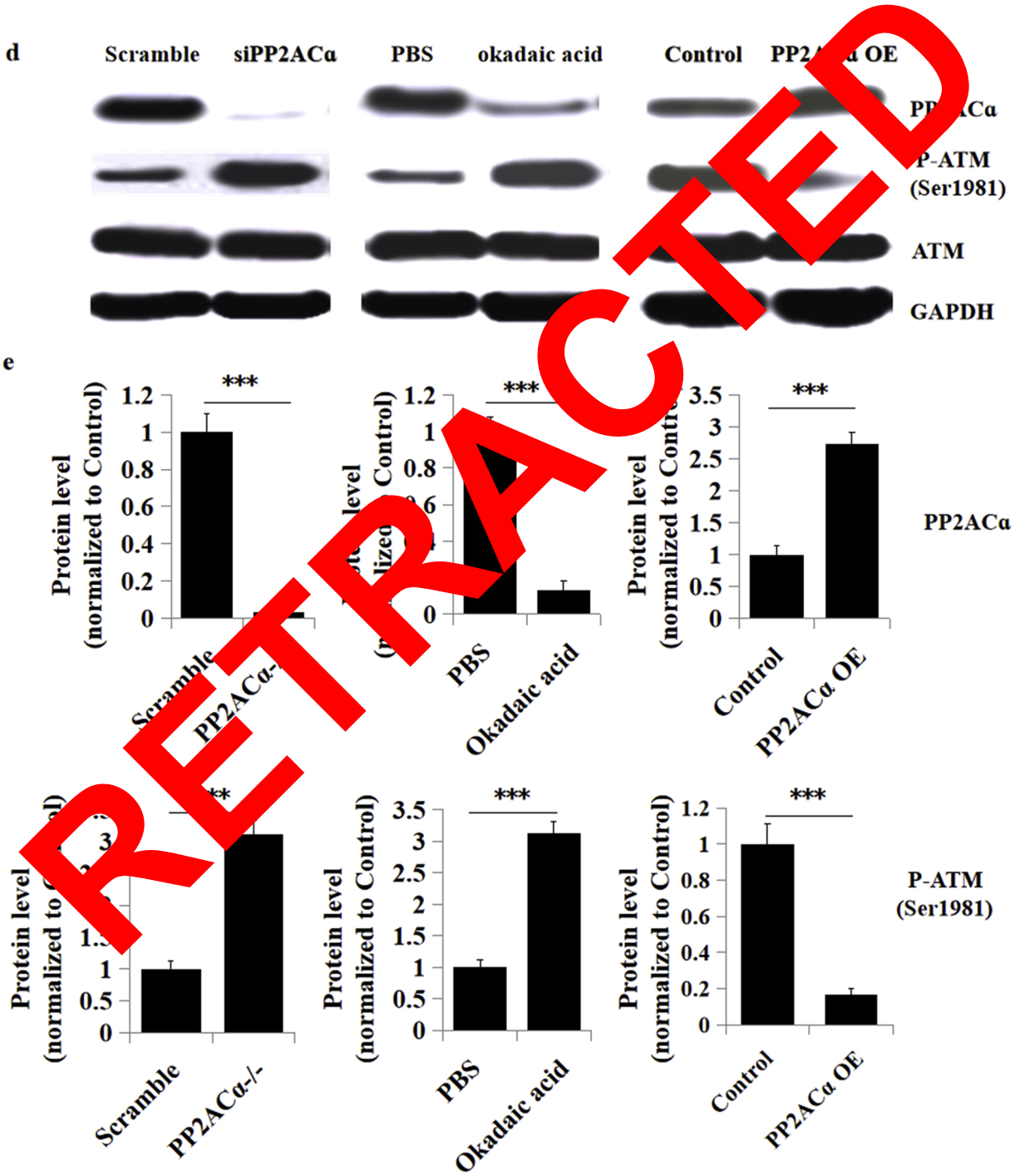

Fig. 5. (*continued*)

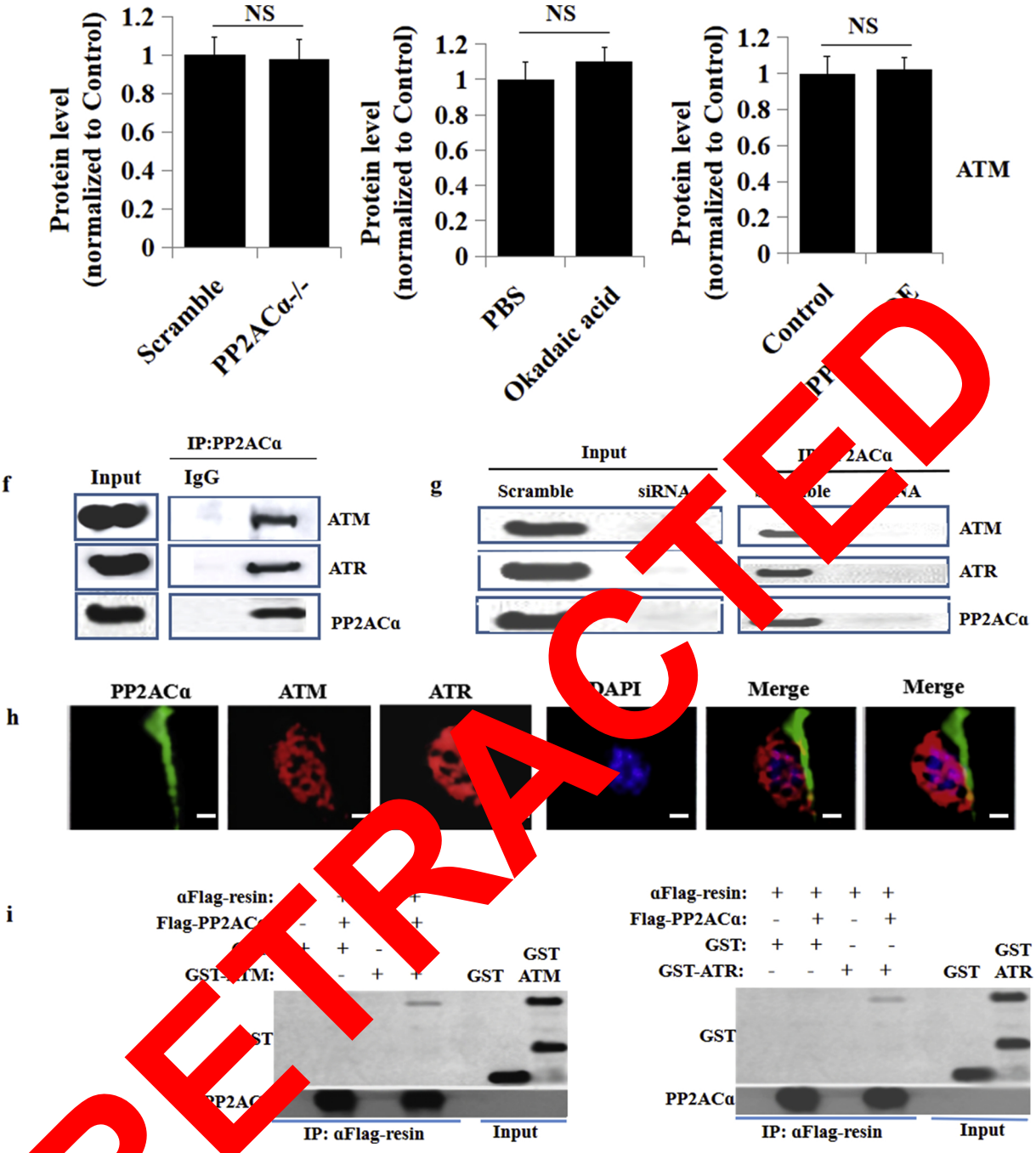

Fig. 5. (*continued*)

McCright et al., 1 Whether HIC1 was involved in DNA repair was poorly understood. aracterize the function of HIC1 in DNA damage response, we mea ured the co-localization of HIPK2 and γH2AX, in the nuclei of the HICI-deficient neuroprogenitor cells subjected to 4Gy IR stimuli. Notably, deletion of HIC1 resulted in a down-regulation in DNA damage response, as indicated by the decreased co-localization of HIPK2 and γH2AX foci (Fig. 7a).

Since γH2AX is considered as a classical molecule for sensing and localizing DNA damage sites, therefore, co-localization of γH2AX and HIPK2 in nuclei indicated their synergistic roles in DNA damage response. Deletion of HIC1 resulted in the compromised reactivity of γH2AX/HIPK2 in nuclei, implying that HIC1 functioned as a co-operative partner with HIPK2. Taken together, these findings demonstrated that interactions among the three proteins positively responded to DNA damage in neuroprognitor cells.

3.9. HIC1 directly modulates HIPK2 transcription

As transcriptional factors, P53 and HIC1 may modulate HIPK2 transcription. To test this hypothesis, we performed the chromatin immunoprecipitation (ChIP) assay in 293T cells and WT neuroprogenitor cells. We incubated the precipitated protein-DNA complex with the antibody against HIPK2, and then performed the Real-time PCR assay to quantify HIPK2 DNA templates. Several independent experiments finally revealed that HIC1 directly bind to *Hipk2* gene promoter in 293T cells and neuroprogenitor cells (Fig. 7b). Upon DNA damage stimuli (5Gy IR), binding efficiency of HIC1 at *HIPK2* gene promoter was largely improved (Fig. 7b).

To confirm this finding, we first transfected *Hic1* gene with HIPK2 luciferase reporter constructs into the two types of cells, and then measured HIPK2 promoter activity. As expected, over-expression of

Hic1 gene resulted in the significant enhancement of HIPK2 luciferase activity in the two types of cells (Fig. 7c). These findings indicated that HIC1 played a direct transcriptional regulatory role in *Hipk2* gene expression in 293T cells and neuroprogenitor cells. However, P53 was not found to transcriptionally modulate *Hipk2* gene expression in the two types of cells (data not shown).

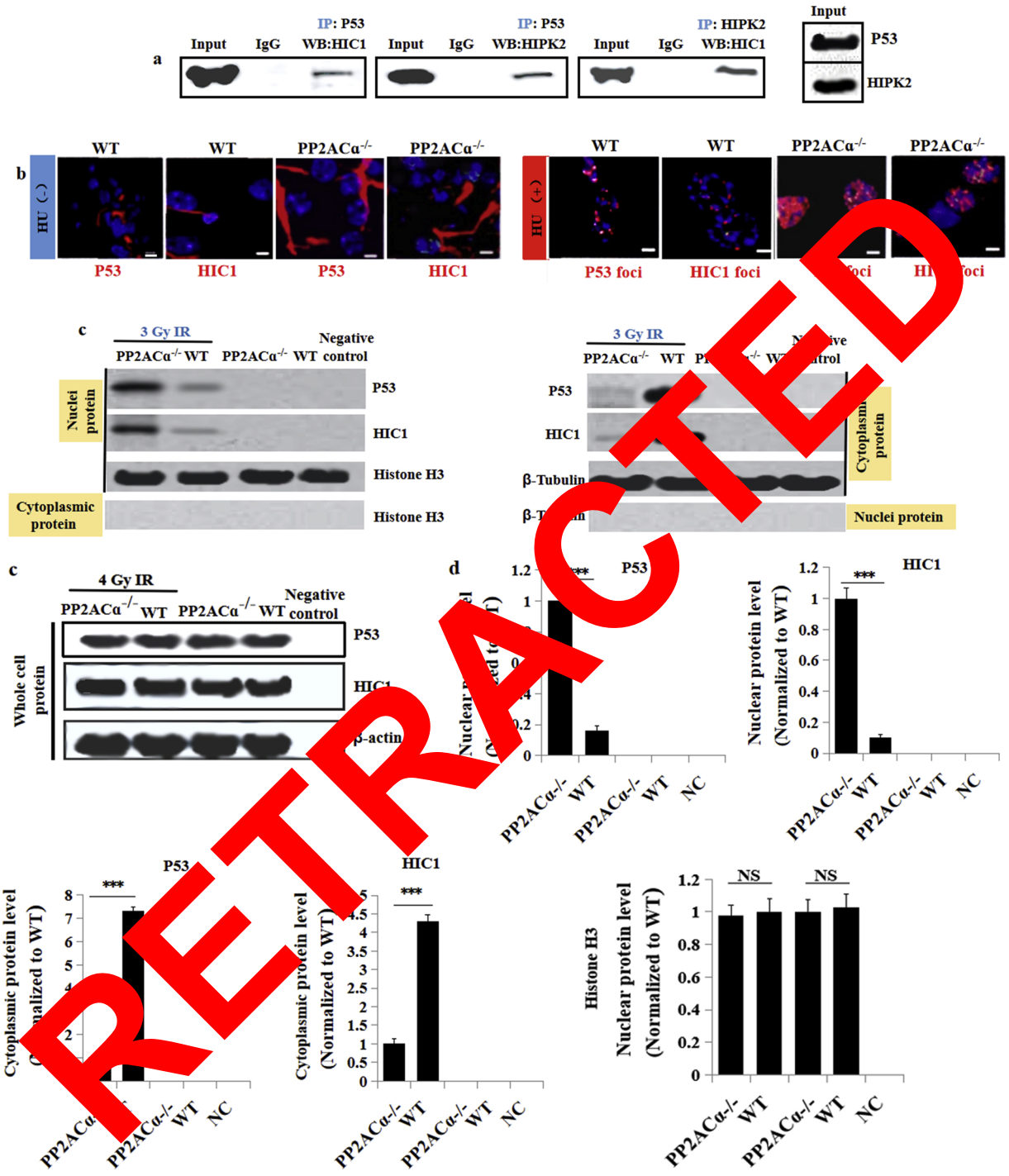

Fig. 6. PP2ACα deletion promotes P53/HIC1 nuclei translocation.
a) Co-immunoprecipitation assay on P53/HIIC1, P53/HIPK2 and HIIC1/HIPK2 in the cytoplasmic extracts from the WT neuroprogenitor cells subjected to 4Gy IR. siP53: siRNA-mediated P53 knock-down; siHIC1: siRNA-mediated HIC1 knock-down. **b)** Immunofluorescent assay of co-expressions of P53 and HIC1 in the WT neuroprogenitor cells treated with or without HU. Phalloidin staining (red), DAPI staining (blue). Scale bar represents 50 μm (left panel) and 10 μm (right panel). **c)** Immunoreactivities of nuclear, cytoplasmic and whole P53, HIC1, Histone H3 and β-actin were measured in the neuroprogenitor cells (stimulated with or without 4Gy IR) by immunoblotting assay. Negative control (NC): without incubation with the primary antibody against P53 or HIC1. **d)** Quantitation of immunoreactivities of P53, HIC1, Histone H3 and β-Tubulin. ***$p < 0.001$ VS. WT, *t*-test, n = 10. **e)** Immunoreactivities of P53, HIC1 and HIPK2 were measured in the nuclei extracts from the treated neuroprogenitor cells by immunoblotting assay. **f)** Quantitation of immunoreactivities of P53, HIC1 and HIPK2. ***$p < 0.001$ VS. WT, *t*-test, n = 10. **g)** Immunoblotting assay of ATR and phosphorylated-p53 (Ser15) in the treated WT neuroprogenitor cells. siATR: siRNA-mediated ATR knock-down. **h)** Quantitation of immunoreactivities of ATR and phosphorylated-p53 (Ser15). ***$p < 0.001$ VS. WT, *t*-test, n = 10. Bar graphs represent means ± S.D. of experimental triplicates.

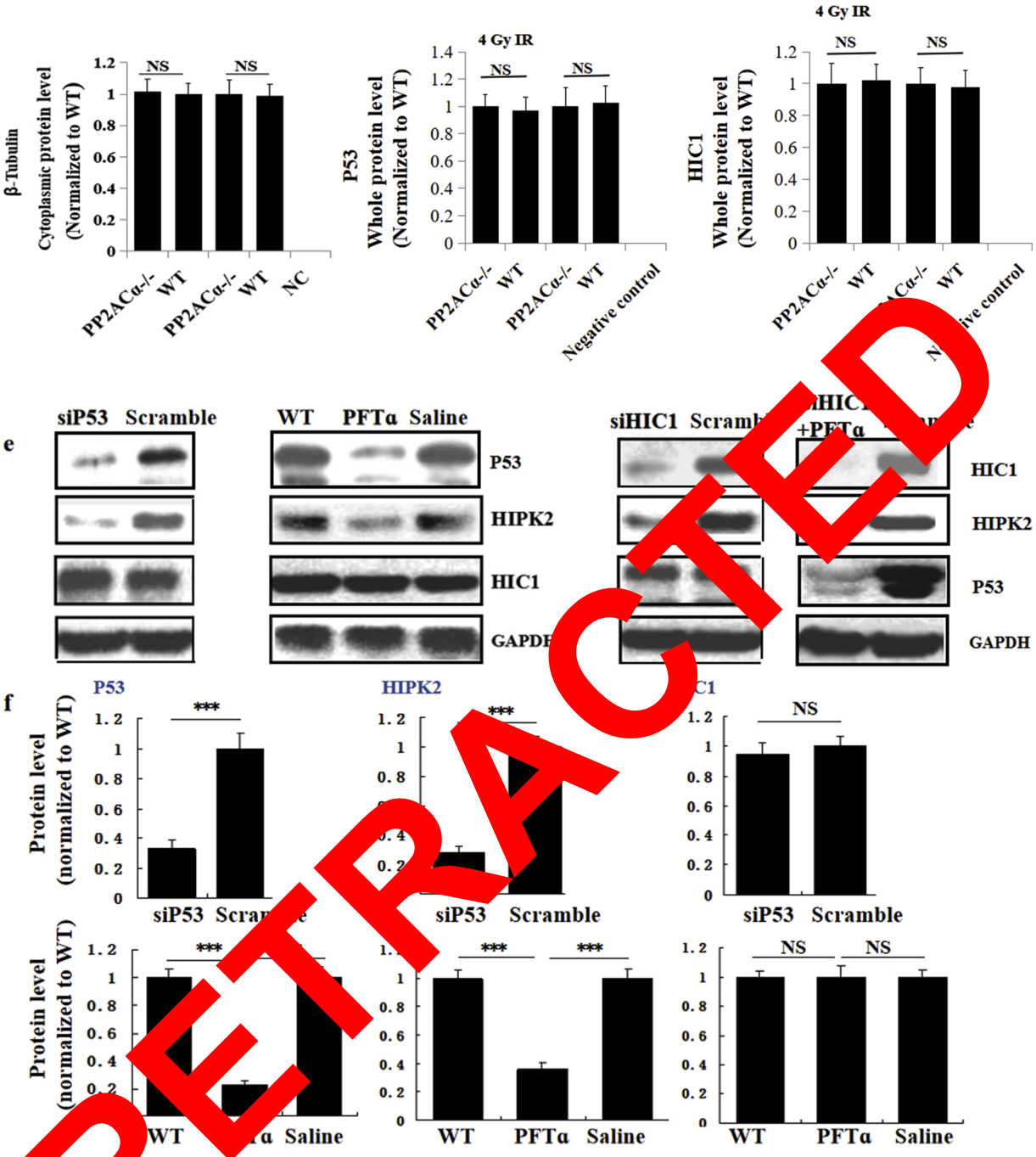

Fig. 6. (*continued*)

4. Discussion

Brain development is known to be regulated in a precise spatio-temporal manner. In the present study, our study demonstrates that PP2ACα is a newly found regulatory factor for mouse brain development during embryonic and postnatal stage. PP2ACα protein deficiency results in DNA damage exhibited in the form of SSB, which initiates the ATR/CHK1 cascade in neocortex and neuroprogenitor cells. PP2ACα can directly associate with ATM and ATR at protein level, and it plays an essential regulatory role in the de-phosphorylation of ATM and ATR in normal neuroprogenitor cells. Notably, P53, HIC1 and HIPK2 co-ordinately respond to DNA damage in the nuclei of neuroprogenitor cells. P53/HIC1 function complex will be translocated into nuclei and interacts with HIPK2/γH2AX at the sites of DNA strand breaks. Notably, HIC1 plays a direct transcriptional regulatory role in HIPK2 gene expression.

PP2A is a conserved protein serine/threonine phosphatase that functions as a trimeric protein complex consisting of a catalytic subunit (PP2Ac or C), a scaffold subunit (PR65 or A), and an alternative regulatory B subunits. In mammals, A and B isoforms are the essential elements of both the catalytic (C) and scaffolding (PR65/A) subunits. B subunit families consist of four members, each with several isoforms or splice variants. The variable composition in PP2A protein structure guarantees a vast array of specific substrates. The complicated regulatory roles of PP2A in neurodegenerative disease have been well studied in previous studies (Lyu et al., 2013; Mayer et al., 1991; Santoro et al., 1998; Shenolikar, 1994; McCright et al., 1996; Inoue et al., 1999; Kawabe et al., 1997; Kins et al., 2003; Louis et al., 2011; Kamibayashi and Mumby, 1995; Oliver and Shenolikar, 1998; Alonso et al., 2004; Millward et al., 1999; Sontag et al., 1995; Barford, 1996; Bononi et al.,

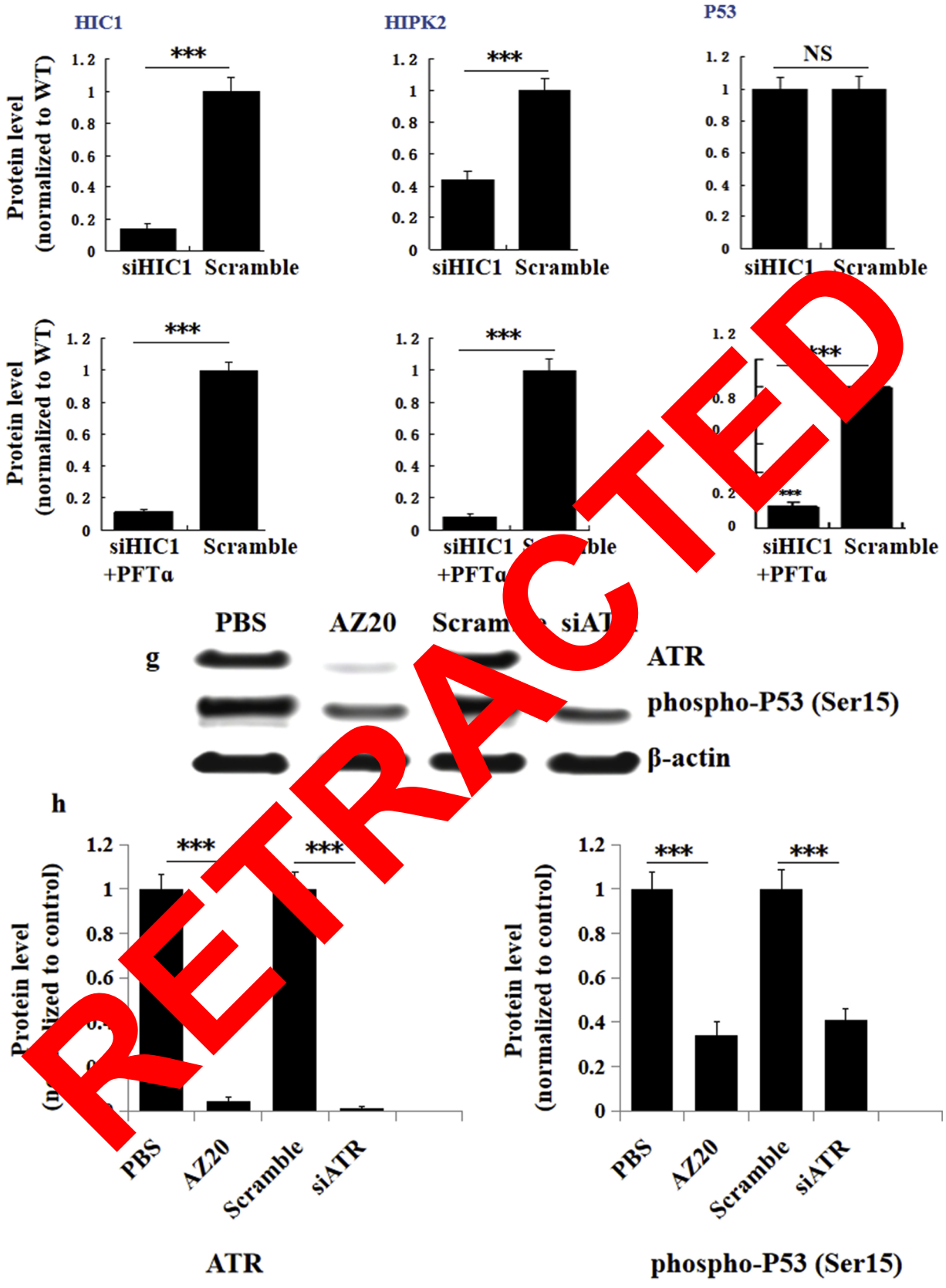

Fig. 6. (*continued*)

2011; Mumby and Walter, 1993; Chen et al., 2016; Lucas and Armstrong, 2015; Janssens and Goris, 2001; Okamoto et al., 1996).

In Alzheimer disease (AD) study, it has been reported that alteration in PP2A catalytic activity and abnormality in PP2A phosphorylation are localized in the AD-affected regions. Hyperphosphorylation of Tau protein, amyloidogenesis and synaptic deficits in the CNS neuronal cells are studied as the decisive contributors to the pathogenesis of AD (Sontag et al., 1995; Barford, 1996; Bononi et al., 2011; Mumby and

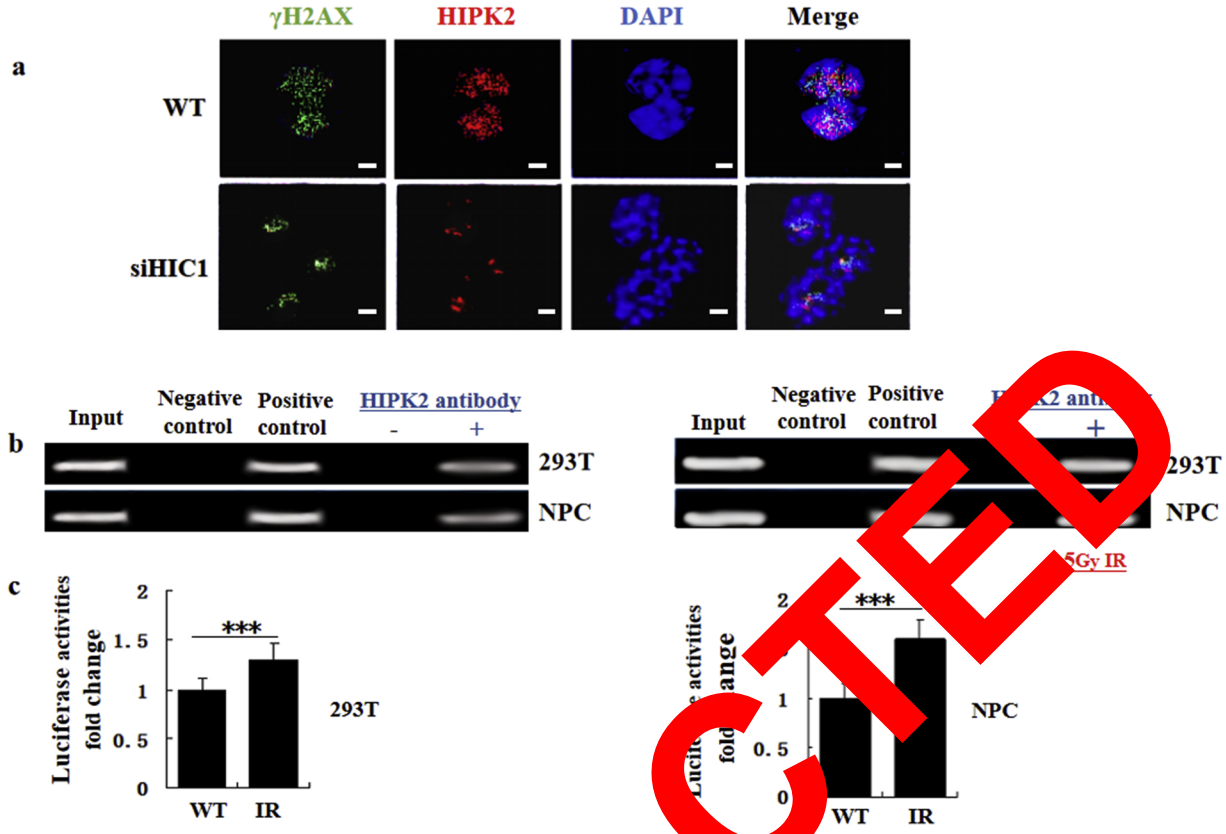

Fig. 7. Interplay among p53, HIC1 and HIPK2 in response to DNA dama
a) Co-localization of γH2AX and HIPK2 were measured in the nuclei o neuroprogenitor cells by immunofluorescent assay. Alexa staining (green), phalloidin staining (red), DAPI staining (blue). Scale bar represents 5 μm Chi binding activity of HIC1 to *Hipk2* promoter in 293T cells and WT neuroprogenitor cells. **c)** Luciferase activity assay in 293T cells and WT neu or cells subjected to 5Gy IR. ***$p < 0.001$ VS. WT, *t*-test, n = 10. Bar graphs represent means ± S.D. of experimental triplicates.

Walter, 1993; Chen et al., 2016; Lucas and Arm g, 201 anssens and Goris, 2001; Okamoto et al., 1996). PP2A Bα is tau phosphatase, controls Tau phosphory n. Dist n of the interaction between PP2A/Bα and tau co fes to tau de ulation in AD (Sontag et al., 1995; Barford, 199 on et al., 2011; mby and Walter, 1993; Chen et al., 2016; ucas and A ong, 2015; Janssens and Goris, 2001; Okamoto et 996).

HIC1, an epigenetically gulated transcriptional repressor, functionally cooperates with p53 to sup s age-dependent development of cancer in mice. HIC1 enco c-finger nscriptional factor that represses the trans n of t r cell ough two autonomous repression domai et al., 002; Dhordain et al., 1997). HIPK2, as a ine-thr ine kina initially identified through its ability to in t w homeoprotein, mediates the phosphorylation of P esponse to UV irradiation, which was responsible for P53-mediated a otic activity (Kim et al., 1998; Hofmann et al., 2002; D'Orazi et al., 2).

However, the roles of PP2A in DNA repair especially during embryonic period were poorly understood. The molecular links among PP2A, ATM, ATR, P53, HIC1 and HIPK2 in DNA repair mechanisms underlying neurogenesis was unknown. Brain development during embryonic period is a strictly regulated process. During this process, neural stem cells originated from the ventricular zone will rapidly proliferate during cell cycle progression and they will migrate to cerebral cortical zone to form neocortex. Because of rapid proliferating features in neural stem cells, high level of oxidative stress and DNA damage will be generated and accumulated at replication forks. According to previous studies, several pathways may execute to recognize and repair DNA lesions at replication forks. Unrepaired DNA strand breaks can cause detrimental outcome such as chromosomal instability, growth retardation, cell death, developmental defects, neurodegeneration and neoplastic transformation (Riches et al., 2008; Lee and Paull, 2005; Difilippantonio and Nussenzweig, 2007; Jazayeri et al., 2008; D' Amours and Jackson, 2002; Stracker and Petrini, 2011; Stiff et al., 2005).

In our previous study, we observed that *Pp2acα* gene knock-down in the CNS neuronal cells resulted in cortical developmental deficit, which impaired mouse's cognitive integrity (Liu et al., 2018). Subsequently, we explored the molecular mechanism underlying cortical developmental deficit, and found that *Pp2acα* gene knock-out initiates the Hippo cascade in cortical neuroprogenitor cells, which blocked the translocation of YAP into nuclei, contributing to the decreased cellular proliferation and protein synthesis (Liu et al., 2018).

Here, our study by using the *PP2ACα*$^{-/-}$ mice models provides the direct evidence that PP2ACα deletion impaired the structural organization in neocortex and cerebella, as a consequence of activated apoptotic response triggered by the over-loaded DNA damage during neurogenesis. In neuroprogenitor cells, endogenous DNA damage, resulting from PP2ACα deletion, yielded an up-regulation in ATR phosphorylation activity, suggesting that PP2ACα participates in DNA single strand break (SSB) repair through the ATR/Chk1 cascade. As shown in the co-immunoprecipitation assay, PP2ACα protein' interaction with ATM or ATR was first identified in neuroprogenitor cells and 293T cells suffering from DNA damage. We consider that PP2ACα is capable of activating the ATM/ATR repair cascade in the dividing neurons. However, DNA damage will disrupt the silence of ATM/ATR and promote the phosphorylation of the two proteins, which triggers P53-mediated apoptotic response in cells. The functional balances between protein kinase (ATM/ATR) and protein phosphatase (PP2ACα) maintain the stability of DNA strands in neuroprogenitor cells.

In previous study, we report that P73, directly targeted by the Hippo cascade, can bind to the promoter of glutaminase2 (GLS2) that plays a dominant role in the enzymatic regulation in glutamate/glutamine cycle. And *Pp2aca* gene knock-out suppresses the glutamine synthesis through up-regulating the phosphorylation activity of P73 in cortical NPCs, implying that PP2ACα indirectly modulates the glutamine synthesis of cortical NPCs through targeting P73 that plays a regulatory role in GLS2 transcription (Liu et al., 2018).

In this study, we first report that P53, HIC1 and HIPK2 co-operatively respond to DNA damage in neuroprogenitor cells. The interaction among the three proteins has been confirmed in the nuclei extracts of neuroprogenitor cells by co-immunoprecipitation assay. Without DNA damage, P53 and HIC1 are co-expressed in the cytoplasm of normal neuroprogenitor cells. As the occurrence of DNA damage, two proteins will be translocated into nuclei and form foci at the sites of DNA strand breaks. PP2ACα deficiency, as an activator to DNA damage response, promotes the translocation of P53 and HIC1 into nuclei and induces them to form strong foci at the sites of DNA damage. Co-localization of HIPK2 and γH2AX at the sites of replication fork blockages confirms the role of HIPK2 in sensing DNA damage. Therefore, HIPK2 owns the potential to be developed as a new DNA damage marker in neuronal cells.

Notably, HIC1, as a transcriptional factor, can directly bind to *Hipk2* gene promoter in 293T cells and neuroprogenitor cells, indicating the direct transcriptional regulatory role of HIC1 in *Hipk2* gene expression. Previous studies have reported that HIPK2 can directly modulate P53 phosphorylation, which can be considered as a feedback modulation mechanism on P53-mediated apoptotic signal (Hofmann et al., 2002; D'Orazi et al., 2002). Based on this finding, we propose that P53, HIC1 and HIPK2 may form a regulation loop in nuclei and the interplay among the three proteins will augment the apoptotic cascade i neuronal stem cells with over-loaded DNA damage.

In the future study, we will focus on investigating whether ot protein molecules are involved in the initiation the PP2ACα-ATR-P cascade in neuroprogenitor cells. We will deeply expl olecula mechanisms underlying the P53-mediated HIC1 a HIPK regula-tions in response to DNA damage, and will inv te wh ther proteins can assist with P53 to modulate HI and activi

5. Conclusions

Our findings reveal that PP2 Cα plays a ective role in brain development through maint g DNA stabilit neuroprojenitor cells. HIC1, as a down-stre execut of the ATR/ATM cascade, will be translocated into nu with purpose to interact with the HIPK2/γH2AX complex, an by sens NA damage sites. HICI plays a direct tran nal re tory in *Hipk2* gene expression. The interplay g t 53/HI K2 regulation loop maintains DNA stabilit neuro genitor cel

Author contrib s

B.L., L.L., and W.M designed the research project; B.L. performed the experiments, analyzed the data and wrote the manuscript. L.L performed the experiments and analyzed the data. The other authors performed the experiments, analyzed the data and contributed technical supports.

Conflict of interest

The authors declare that they have no conflict of interest.

Acknowledgements

We appreciate Dr. Man Li and Dr. Qi Zhang (CAMS/PUMC) for technical supports.

References

Alonso, A., Sasin, J., Bottini, N., Friedberg, I., Friedberg, I., Osterman, A., et al., 2004. Protein tyrosine phosphatases in the human genome. Cell 117, 699–711.
Barford, D., 1996. Molecular mechanisms of the protein serine/threonine phosphatases. Trends Biochem. Sci. 21, 407–412.
Bononi, A., Agnoletto, C., De Marchi, E., Marchi, S., Patergnani, S., Bonora, M., et al., 2011. Protein kinases and phosphatases in the control of cell fate. Enzyme Res. 2011, 329098.
Chen, C., Wei, X., Wang, S., Jiao, Q., Zhang, Y., Du, G., et al., 2016. Compression regulates gene expression of chondrocytes through HDAC4 nucleus relocation via PP2A dependent HDAC4 de-phosphorylation. Biochim. Biophys. Acta 1863, 1633–1642.
D' Amours, D., Jackson, S.P., 2002. The Mre11 complex: at the crossroads of DNA repair and checkpoint signaling. Nat. Rev. Mol. Cell Biol. 3, 317–327.
D'Orazi, G., Cecchinelli, B., Bruno, T., Manni, I., Higashimoto, Y., Saito, S., Gostissa, M., Coen, S., Marchetti, A., Del Sal, G., et al., 2002. H domain-interacting protein kinase-2 phosphorylates p53 at Ser 46 and m is. Nat. Cell Biol. 4, 11–19.
Deltour, S., Guerardel, C., Leprince, D., 199 ruitment of S N-CoR-mSin3A-HDAC-repressing complexes is not a gene hanism for B OZ transcriptional repressors: the case of HIC-1 and maFB oc. Natl. A Sci. U. S. A. 96, 14831–14836.
Deltour, S., Pinte, S., Guerardel, C ylyk, B Leprin The human candidate tumor suppressor gene HI ruits C rough a erate GLDLSKK motif. Mol. Cell. Biol. 22, 4890
Dhordain, P., Albagli, O. R. S., Quief Keutz, A., Kerckaert, J.P., Evans, R.M., Leprince, D. Corep SMRT bi e BTB/POZ repressing domain of the LAZ3/BCL6 protein. Proc A ci. U. S. A. 94, 10762–10767.
Difilippantonio, S zweig, A., 200 BS1-ATM connection revisited. Cell Cycle 6, 2 237
Hofmann, T.G., Moller, A. H., Zentgraf, H., Taya, Y., Droge, W., Will, H., Schmitz, M.L., 2002. Regulation activity by its interaction with homeodomain-inter- ein kinase-2. Na Biol. 4, 1–10.
Ino K., Usui, H., Tanabe, O., N ito, Y., Shimizu, M., Takeda, M., 1999. Studies on nctions of the 6 kDa A- and 74-kDa B-(delta)-regulatory subunits in human erythrocyte protei sphatase 2A: dissociation and reassociation of the subunits. J. chem. 126, 1 1135.
Jans V., Goris 001. Protein phosphatase 2A: a highly regulated family of serine/th atases implicated in cell growth and signalling. Biochem. J. 353, 417–43
veri, A., Balestrini, A., Garner, E., Haber, J.E., Costanzo, V., 2008. Mre11-Rad50-pendent processing of DNA breaks generates oligonucleotides that stimulate A activity. EMBO J. 27, 1953–1962.
Kamibayashi, C., Mumby, M.C., 1995. Control of protein phosphatase 2A by multiple families of regulatory subunits. Adv. Prot. Phosphatases 9, 199–214.
Kawabe, T., Muslin, A.J., Korsmeyer, S.J., 1997. HOX11 interacts with protein phosphatases PP2A and PP1 and disrupts a G2/M cell-cycle checkpoint. Nature 385, 454–458.
Kim, Y.H., Choi, C.Y., Lee, S.J., Conti, M.A., Kim, Y., 1998. Homeodomain-interacting protein kinases, a novel family of co-repressors for homeodomain transcription factors. J. Biol. Chem. 273, 25875–25879.
Kins, S., Kurosinski, P., Nitsch, R.M., Gotz, J., 2003. Activation of the ERK and JNK signaling pathways caused by neuron-specific inhibition of PP2A in transgenic mice. Am. J. Pathol. 163, 833–84310.
Lee, J.H., Paull, T.T., 2005. ATM activation by DNA double-strand breaks through the Mre11-Rad50-Nbs1 complex. Science 308, 551–554.
Liu, B., Li, H.S., Huang, Y.F., Guo, L.J., Luo, L.S., 2018. Protein phosphatase 2ACα gene knock-out results in cortical atrophy through activating hippo cascade in neuronal progenitor cells. Int. J. Biochem. Cell Biol. 95, 53–62.
Louis, J.V., Martens, E., Borghgraef, P., Lambrecht, C., Sents, W., Longin, S., et al., 2011. Mice lacking phosphatase PP2A subunit PR61/B'delta (Ppp2r5d) develop spatially restricted tauopathy by deregulation of CDK5 and GSK3beta. Proc. Natl. Acad. Sci. 108, 6957–6962.
Lucas, S.J., Armstrong, D.L., 2015. Protein phosphatase modulation of somatostatin receptor signaling in the mouse hippocampus. Neuropharmacology 99, 232–241.
Lyu, J., Kim, H.R., Yamamoto, V., Choi, S.H., Wei, Z., Joo, C.K., Lu, W., 2013. Protein phosphatase 4 and Smek complex negatively regulate Par3 and promote neuronal differentiation of neural stem/progenitor cells. Cell Rep. 14, 593–600.
Mayer, R.E., Khew-Goodall, Y., Stone, S.R., Hemmings, B.A., 1991. Structure and expression of protein phosphatase PP2A. Adv. Prot. Phosphatases 6, 125–143.
McCright, B., Rivers, A.M., Audlin, S., Virshup, D.M., 1996. The B56 family of protein phosphatase 2A (PP2A) regulatory subunits encodes differentiation-induced phosphoproteins that target PP2A to both nucleus and cytoplasm. J. Biol. Chem. 271, 22081–22089.
Millward, T.A., Zolnierowicz, S., Hemmings, B.A., 1999. Regulation of protein kinase cascades by protein phosphatase 2A. Trends Biochem. Sci. 24, 86–91.
Mumby, M.C., Walter, G., 1993. Protein serine/threonine phosphatases: structure, regulation and functions in cell growth. Physiol. Rev. 73, 673–692.
Okamoto, K., Kamibayashi, C., Serrano, M., Prives, C., Mumby, M.C., Beach, D., 1996. p53-dependent association between cyclin G and the B-subunit of protein phosphatase 2A. Mol. Cell. Biol. 16, 6593–6602.
Oliver, C.J., Shenolikar, S., 1998. Physiological importance of protein phosphatase inhibitors. Frontiers Biosci. 3, 961–972.
Riches, L.C., Lynch, A.M., Gooderham, N.J., 2008. Early events in the mammalian response to DNA double-strand breaks. Mutagenesis 23, 331–339.

Santoro, M.F., Annard, R.R., Robertson, M.M., Peng, Y.W., Brady, M.J., Mankovich, J.A., Hacket, M.C., Ghayur, T., Walter, G., Wong, G.G., Giegel, D.A., 1998. Regulation of protein phosphatase 2A activity by caspase-3 during apoptosis. J. Biol. Chem. 273, 13119–13128.
Shenolikar, S., 1994. Protein serine/threonine phosphatases-new avenues for cell regulation. Annu. Rev. Cell Biol. 63, 55–86.
Sontag, E., Nunbhakdi-Craig, V., Bloom, G.S., Mumby, M.C., 1995. A novel pool of protein phosphatase 2A is associated with microtubules and is regulated during the cell cycle. J. Cell Biol. 128, 1131–1144.
Stiff, T., Reis, C., Alderton, G.K., Woodbine, L., O'Driscoll, M., Jeggo, P.A., 2005. Nbs1 is required for ATR- dependent phosphorylation events. EMBO J. 24, 199–208.
Stracker, T.H., Petrini, J.H., 2011. The MRE11 complex: starting from the ends. Nat. Rev. Mol. Cell Biol. 12, 90–103.